EUROPEAN SCHOOL OF MOLECULAR MEDICINE

NAPLES SITE

UNIVERSITA' DEGLI STUDI DI NAPOLI

"FEDERICO II"

Ph.D. in Molecular Medicine – Ciclo III/XXI

Human Genetics

"IDS crossing of the Blood-Brain Barrier corrects CNS defects in MPSII mice"

Tutor:
Dr. Maria Pia Cosma

Internal Supervisor:
Prof. Andrea Ballabio

External Supervisor:
Prof. Mark Haskins

Coordinator:
Prof. Francesco Salvatore

Ph.D. student:
Vinicia Assunta Polito

Academic Year: 2008-2009

TABLE OF CONTENTS:

7. RT-PCR
8. Quantitative real-time PCR
9. Quantitative analysis of GAG accumulation in the urine
10. Open-field test
11. Statistical analysis

RESULTS

1. Knock-out mouse model of Hunter syndrome
2. IDS gene delivery in the MPSII mice
3. Rescue of the IDS activity in the tissues and in the brain of adult MPSII mice by AAV2/5CMV-hIDS
4. Clearance of the lysosomal GAG accumulation in the tissues and in the urine of treated MPSII mice
5. Characterization and complete correction of the brain defects in the treated MPSII mice
6. Crossing of Blood-Brain Barrier (BBB) by IDS enzyme
7. Corrections of the locomotor defects in the treated MPSII mice and their performance at the open-field test

DISCUSSION

REFERENCES

AKNOWLEDGEMENTS

LIST OF ABBREVIATIONS:

MPSII: Mucopolysaccharidosis type II

IDS: Iduronate-2-sulfatase

GAG: Glycosaminoglycan

BBB: Blood-Brain Barrier

M6PR: Mannose-6-phosphate receptor

FIGURES INDEX:

ABSTRACT

Mucopolysaccharidosis type II (MPSII), or Hunter syndrome, arises from a deficiency in iduronate 2-sulfatase (IDS), and it is characterized by progressive somatic and neurological involvement. The MPSII mouse model reproduces the features of MPSII patients. Systemic administration of the AAV2/5CMV-hIDS vector in MPSII mouse pups results in the full correction of glycosaminoglycan (GAG) accumulation in visceral organs and in the rescue of the defects and GAG accumulation in the central nervous system (CNS). Remarkably, in treated MPSII animals, this CNS correction arises from the crossing of the blood-brain barrier by the IDS enzyme itself, not from the brain transduction. Thus, I show in this thesis that early treatment of MPSII mice with one systemic injection of AAV2/5CMV-hIDS results in prolonged and high levels of circulating IDS that can efficiently and simultaneously rescue both visceral and CNS defects for up to 18 months after therapy.

INTRODUCTION

1. BIOSYNTHESIS OF LYSOSOMAL ENZYMES

Newly synthesized glycoproteins originating from the rough ER pass through the Golgi stacks and are then sorted to various destinations. Along this route, lysosomal enzymes are recognized by GlcNAc-P-T and phosphorylated in the intermediate compartment (*cis*-Golgi network; CGN) and then acted upon by "uncovering" enzyme (phosphodiester glycosidase) in the *trans*-Golgi network (TGN). Beyond the TGN, trafficking of lysosomal enzymes is primarily mediated by the MPRs through early endosomes to late endosomes, in which their lysosomal enzyme cargo is released. Smaller amounts of lysosomal enzymes can escape capture by MPRs and be secreted into the extracellular fluid. Lysosomal enzymes can also reenter the cell by binding to cell-surface MPRs and subsequent endocytosis (Figure 1) [1-3]. Once in the endocytic pathway, internalized lysosomal enzymes can intermingle with those following the biosynthetic route, as depicted. Additional pathways for MPRs include recycling from the early endosome to the cell surface and back to the TGN, and from the recycling endosome and the late endosome, following release of their lysosomal enzyme cargo.

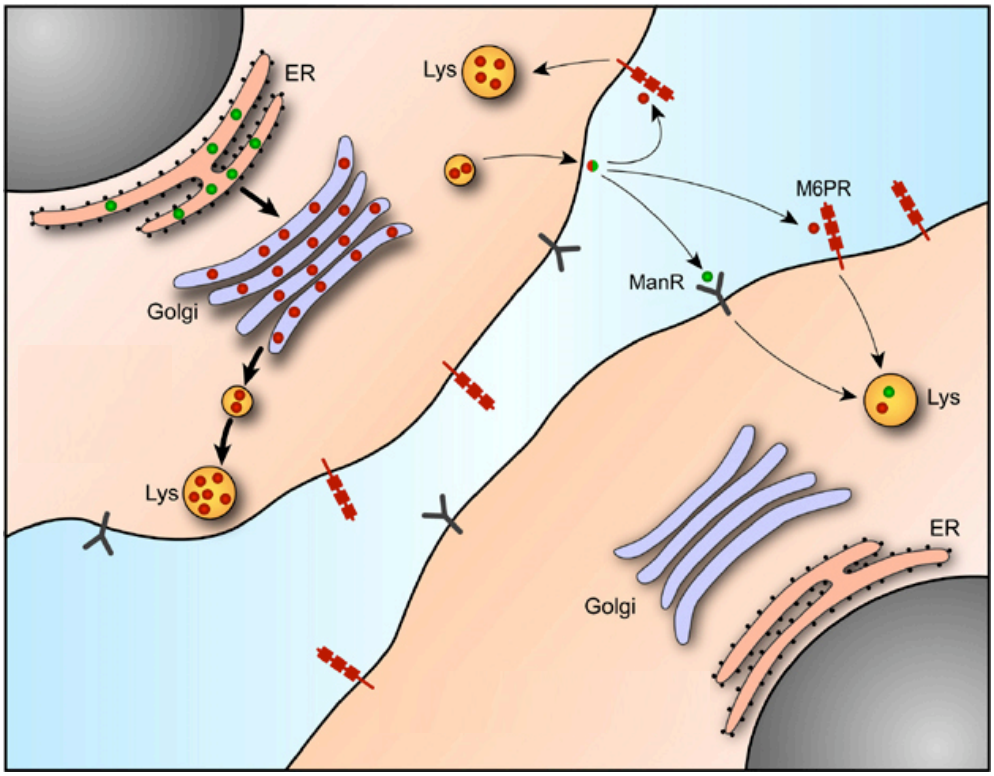

Figure 1. Biosynthesis and localization of lysosomal enzymes through the internal and external pathways of mannose-6-phosphate receptor

Nascent lysosomal enzymes are glycosylated (green circles) in the endoplasmic reticulum (ER) of cells. The enzymes then acquire the mannose 6-phosphate modification (red circles) in the Golgi apparatus (Golgi) where they bind the mannose 6-phosphate receptor (M6PR). The majority (heavy arrows) of the enzymes are then trafficked to the mature lysosome (Lys). A minority (fine arrows) of the lysosomal enzymes are secreted from the cell. Extracellular phosphorylated or nonphosphorylated enzyme can bind the plasma membrane-localized M6PR or the mannose receptor (ManR), respectively. Both receptors mediate the endocytosis and subsequent lysosomal targeting of the exogenous enzymes.

2. LYSOSOMAL STORAGE DISEASES (LSD)

Lysosomal storage diseases (LSDs) are a group of approximately 40 rare inherited metabolic disorder that result from defects in lysosomal function. Lysosomal storage diseases result when a specific organelle in the cells of body– the lysosome – malfunctions [4]. Lysosomal storage disorders are caused by lysosomal dysfunction usually as a consequence of deficiency of a single

enzyme required for the metabolism of lipids, glycoproteins (sugar containing proteins) or so-called mucopolysaccharides. Individually, LSDs occur with incidences of less than 1:100.000, however, as a group the incidence is about 1:5000 - 1:10.000 [5-8]. Most of these disorders are autosomal recessively inherited [5], however a few are X-linked recessively inherited, such as Fabry diseases and Hunter syndrome (MPS II). The lysosome is commonly referred to as the cell's recycling center because it processes unwanted material into substances that the cell can utilize. Lysosomes break down this unwanted matter via enzymes, highly specialized proteins essential for survival. Lysosomal disorders are triggered when a particular enzyme exists in too small an amount or is missing altogether. When this happens, substances accumulate in the cell. In other words, when the lysosome doesn't function normally, excess products destined for breakdown and recycling are stored in the cell. Like other genetic diseases, individuals inherit lysosomal storage diseases from their parents. Although each disorder results from different gene mutations that translate into a deficiency in enzyme activity, they all share a common biochemical characteristic – all lysosomal disorders originate from an abnormal accumulation of substances inside the lysosome. Lysosomal storage diseases affect mostly children and they often die at a young and unpredictable age, many within a few months or years of birth. Many other children die of this disease following years of suffering from various symptoms of their particular disorder.

The symptoms of lysosomal storage disease vary, depending on the particular disorder and other variables like the age of onset, and can be mild to severe. They can include developmental delay, movement disorders, seizures, dementia deafness and/or blindness. Some people with lysosomal storage disease have enlarged livers (hepatomegaly) and enlarged spleens (splenomegaly), pulmonary and cardiac problems, and bones that grow abnormally. The lysosomal storage diseases are generally classified by the nature of the primary stored material involved, and can be broadly broken into the following:

- Lipid storage disorders, mainly sphingolipidoses (including Gaucher's and Niemann-Pick disease)
    - gangliosidosis (including Tay-Sachs disease)
    - leukodystrophies
- mucopolysaccharidoses (including Hunter syndrome and Hurler disease)
- glycoprotein storage disorders
- mucolipidoses

3. MUCOPOLYSACCHARIDOSES (MPSs)

Mucopolysaccharidoses are a group of metabolic disorders caused by the absence or malfunctioning of lysosomal enzymes needed to break down molecules called glycosaminoglycans - long chains of sugar carbohydrates in each of our cells that help build bone, cartilage, tendons, corneas, skin and

connective tissue. Glycosaminoglycans (formerly called mucopolysaccharides) are also found in the fluid that lubricates our joints. Glycosaminoglycans (GAGs) or mucopolysaccharides are long unbranched polysaccharides consisting of a repeating disaccharide unit. The repeating unit consists of a hexose (six-carbon sugar) or a hexuronic acid, linked to a hexosamine (six-carbon sugar containing nitrogen). Protein cores made in the rough endoplasmic reticulum are posttranslationally modified by glycosyltransferase in the Golgi apparatus, where GAG disaccharides are added to protein cores to yield proteoglycans. This family of carbohydrates is essential or important for life. GAGs form an important component of connective tissues. GAG chains may be covalently linked to a protein to form proteoglycans. Some examples of glycosaminoglycan uses in nature include heparin as an anticoagulant, hyaluronan as a component in the synovial fluid lubricant in body joints, and chondroitins which can be found in connective tissues, cartilage and tendons. People with a mucopolysaccharidosis either do not produce enough of one of the 11 enzymes required to break down these sugar chains into simpler molecules, or they produce enzymes that do not work properly. Over time, these glycosaminoglycans collect in the cells, blood and connective tissues. The result is permanent, progressive cellular damage which affects appearance, physical abilities, organ and system functioning, and, in most cases, mental development. The mucopolysaccharidoses are part of the lysosomal storage disease family,

that result when a specific organelle in our body's cells – the lysosome – malfunctions. The lysosome is commonly referred to as the cell's recycling center because it processes unwanted material into substances that the cell can utilize. Lysosomes break down this unwanted matter via enzymes, highly specialized proteins essential for survival. Lysosomal disorders like mucopolysaccharidosis are triggered when a particular enzyme exists in too small an amount or is missing altogether. The mucopolysaccharidoses share many clinical features but have varying degrees of severity. These features may not be apparent at birth but progress as storage of glycosaminoglycans affects bone, skeletal structure, connective tissues, and organs. Neurological complications may include damage to neurons as well as pain and impaired motor function. This results from compression of nerves or nerve roots in the spinal cord or in the peripheral nervous system, the part of the nervous system that connects the brain and spinal cord to sensory organs such as the eyes and to other organs, muscles, and tissues throughout the body. Depending on the mucopolysaccharidosis subtype, affected individuals may have normal intellect or may be profoundly retarded, may experience developmental delay, or may have severe behavioral problems. Many individuals have hearing loss, either conductive (in which pressure behind the ear drum causes fluid from the lining of the middle ear to build up and eventually congeal), neurosensitive (in which tiny hair cells in the inner ear are damaged), or both. Communicating

hydrocephalus — in which the normal circulation of cerebrospinal fluid becomes blocked over time and causes increased pressure inside the head — is common in some of the mucopolysaccharidoses. Surgically inserting a shunt into the brain can drain fluid. The eye's cornea often becomes cloudy from intracellular storage, and glaucoma and degeneration of the retina also may affect the patient's vision. Physical symptoms generally include coarse or rough facial features (including a flat nasal bridge, thick lips, and enlarged mouth and tongue), short stature with disproportionately short trunk (dwarfism), dysplasia (abnormal bone size and/or shape) and other skeletal irregularities, thickened skin, enlarged organs such as liver (hepatomegaly) or spleen (splenomegaly), hernias, and excessive body hair growth. Short and often claw-like hands, progressive joint stiffness, and carpal tunnel syndrome can restrict hand mobility and function. Recurring respiratory infections are common, as are obstructive airway disease and obstructive sleep apnea. Many affected individuals also have heart disease, often involving enlarged or diseased heart valves. Seven distinct clinical types and numerous subtypes of the mucopolysaccharidoses have been identified. Although each mucopolysaccharidosis (MPS) differs clinically, most patients generally experience a period of normal development followed by a decline in physical and/or mental function.

4. SULFATASES AND MSD (MULTIPLE SULFATASE DEFICIT)

Each Mucopolysaccharidosis is caused by an enzymatic deficit of a specific sulfatase.

Sulfatases are hydrolases that cleave sulfate esters from a wide range of substrates, including glycosaminoglycans, sulfolipids, and steroid sulfates [9; 10]. This protein family is represented in most eukaryotes and prokaryotes, with some notable exceptions such as *Saccharomices cerevisiae*. While in prokaryotes sulfatases are involved in sulfur scavenging, in vertebrates they are implicated in the turnover and degradation of sulfated compounds, mostly complex molecules that are hydrolyzed in lysosomes in concert with acidic glycosidases. Functional correlation among sulfatases is reflected in a high degree of amino acid sequence similarity along the entire length of the proteins, suggesting that they have evolved from a common ancestral gene [9; 11]. The three-dimensional structures of two human sulfatases (ARSA and ARSB) were determined, allowing the identification of the sulfatase active site, which contains a highly conserved cysteine residue as part of a metal binding site, closely resembling the active site of alkaline phosphatases [12; 13]. Sulfatases undergo a common and unique posttranslational modification, which is essential for catalytic activity and occurs within the endoplasmic reticulum before the sorting of sulfatases to different cellular compartments. This newly discovered protein modification mechanism, which allows the conversion of the highly

conserved cysteine residue localized at the active site of sulfatases into Cα-formylglycine, has been highly conserved during evolution from bacteria to man [14; 15]. Bacterial sulfatases may have either a cysteine or a serine at their active site, and both of these are modified to formylglycine, albeit by a different protein machinery [16; 17].

To date, thirteen sulfatase genes have been identified in humans [10; 18; 19]. They encode enzymes with different substrate specificity and subcellular localization such as lysosomes, Golgi, and ER [10]. Four of these genes, ARSC, ARSD, ARSE, and ARSF, encoding arylsulfatase C, D, E, and F, respectively, are located within the same chromosomal region (Xp22.3). They share significant sequence similarity and a nearly identical genomic organization, indicating that they arose from duplication events that occurred recently during evolution [11; 20].

The importance of sulfatases in human metabolism is underscored by the identification of at least eight human monogenic diseases caused by the deficiency of individual sulfatase activities [10]. Most of these conditions are lysosomal storage disorders in which phenotypic consequences depend on the type and tissue distribution of the stored material.

Among them are five different types of mucopolysaccharidoses (MPS types II, IIIA, IIID, IVA, and VI) due to deficiencies of sulfatases acting in the catabolism of glycosaminoglycans [4] and metachromatic leukodystrophy (MLD), which is characterized by the storage of sulfolipids in the central and peripheral

nervous systems leading to severe and progressive neurologic deterioration [21]. In addition, two human diseases are caused by deficiencies of non lysosomal sulfatases. These include X-linked ichthyosis, a skin disorder due to steroid sulfatase (STS/ARSC) deficiency, and chondrodysplasia punctata, a disorder affecting bone and cartilage due to arylsulfatase E (ARSE) deficiency [20]. ARSE is also implicated in a drug-induced human malformation syndrome, Warfarin embryopathy, caused by inhibition of the enzymatic activity due to in utero exposure to warfarin during pregnancy [20].

In an intriguing human monogenic disorder, multiple sulfatase deficiency (MSD), all sulfatase activities are simultaneously defective [10; 22; 23]. Consequently, the phenotype of this severe multisystemic disease combines the features observed in individual sulfatase deficiencies. The posttranslational modification which is required for the activity of all sulfatases was found to be defective in a cell line from a patient with MSD, suggesting that this disorder is caused by a mutation in a gene, or genes, implicated in the cysteine-to-formylglycine conversion machinery [14]. In spite of an intense biological and medical interest, efforts aimed at the identification of the MSD gene have been hampered by the rarity of MSD patients and consequent lack of suitable familial cases to perform genetic mapping.

Recently, It has been identified the SUMF1 gene (SUlfatase Modifying Factor 1). SUMF1 encode for a protein that is responsible of activation of all human

sulfatases. The deficit of this gene causes the MSD (Multiple Sulfatase Deficit) [24; 25].

5. MUCOPOLYSACCHARIDOSIS TYPE II (MPSII)

Hunter syndrome, or mucopolysaccharidosis Type II, is a lysosomal storage disease caused by a deficient (or absent) enzyme, iduronate-2-sulfatase (I2S). The syndrome is named after physician Charles A. Hunter (1873-1955), who first described it in 1917. MPS II, is a serious genetic disorder that primarily affects males. It interferes with the body's ability to break down and recycle specific mucopolysaccharides, also known as glycosaminoglycans or GAG. In Hunter syndrome, GAG builds up in cells throughout the body due to a deficiency or absence of the enzyme iduronate-2-sulfatase (I2S). This buildup interferes with the way certain cells and organs in the body function and leads to a number of serious symptoms. As the buildup of GAG continues throughout the cells of the body, signs of Hunter syndrome become more visible. Physical manifestations for some people with Hunter syndrome include distinct facial features, a large head, and an enlarged abdomen. People with Hunter syndrome may also experience hearing loss, thickening of the heart valves leading to a decline in cardiac function, obstructive airway disease, sleep apnea, and enlargement of the liver and spleen. Range of motion and mobility may also be affected. In some cases of Hunter syndrome, central nervous system involvement leads to developmental delays and nervous system problems. Not

all people with Hunter syndrome are affected by the disease in exactly the same way, and the rate of symptom progression varies widely. However, Hunter syndrome is always severe, progressive, and life-limiting.

The visible signs and symptoms of Hunter syndrome (MPS II) in younger people are usually the first clues leading to a diagnosis. In general, the time of diagnosis usually occurs from about 2 to 4 years of age. The most commonly used laboratory screening test for an MPS disorder is a urine test for GAG. It is important to note that the urine test for GAG can occasionally be normal and yet the child still may have an MPS disorder. A definitive diagnosis of Hunter syndrome is made by measuring I2S activity in serum, white blood cells, or fibroblasts from skin biopsy. In some people with Hunter syndrome, analysis of the I2S gene can determine clinical severity. Prenatal diagnosis is routinely available by measuring I2S enzymatic activity in amniotic fluid or in chorionic villus tissue. Since Hunter syndrome is an inherited disorder (X-linked recessive) that primarily affects males, it is passed down from one generation to the next in a specific way. The incidence of Hunter syndrome is estimated to be about 1 in 165,000 male births. The I2S gene is located on the X chromosome. If a male has an abnormal copy of the I2S gene, he will develop Hunter syndrome. A male can obtain an abnormal copy of the I2S gene in one of two ways. His mother is often a carrier; i.e., she has one abnormal and one normal I2S gene, and she passes along the abnormal gene to him. However, during egg and sperm

formation, a mutation can develop in the I2S gene on his X chromosome. In this second case, the mother is not a carrier and the risk of a spontaneous mutation occurring again in a future sibling is low but not zero. Females can carry one abnormal copy of the I2S gene and are usually not affected. In the MPSII patients It has been identified different kind of mutations (point mutation, deletion and insertion) [26], which causes the lack of IDS enzymatic activity. The IDS enzyme takes part in the first catabolic step of dermatan and heparan sulfate [4; 27] (Figure 2).

The human body depends on a vast array of biochemical reactions to support critical functions, including the production of energy, growth and development, communication within the body, and protection from infection. Another critical function is the breakdown of large biomolecules, which is the underlying problem in Hunter syndrome (MPS II) and related storage disorders. The biochemistry of Hunter syndrome is related to a problem in a part of the connective tissue of the body known as the extracellular matrix. This matrix is made up of a variety of sugars and proteins and helps to form the architectural framework of the body. The matrix surrounds the cells of the body in an organized meshwork and functions as the glue that holds the cells of the body

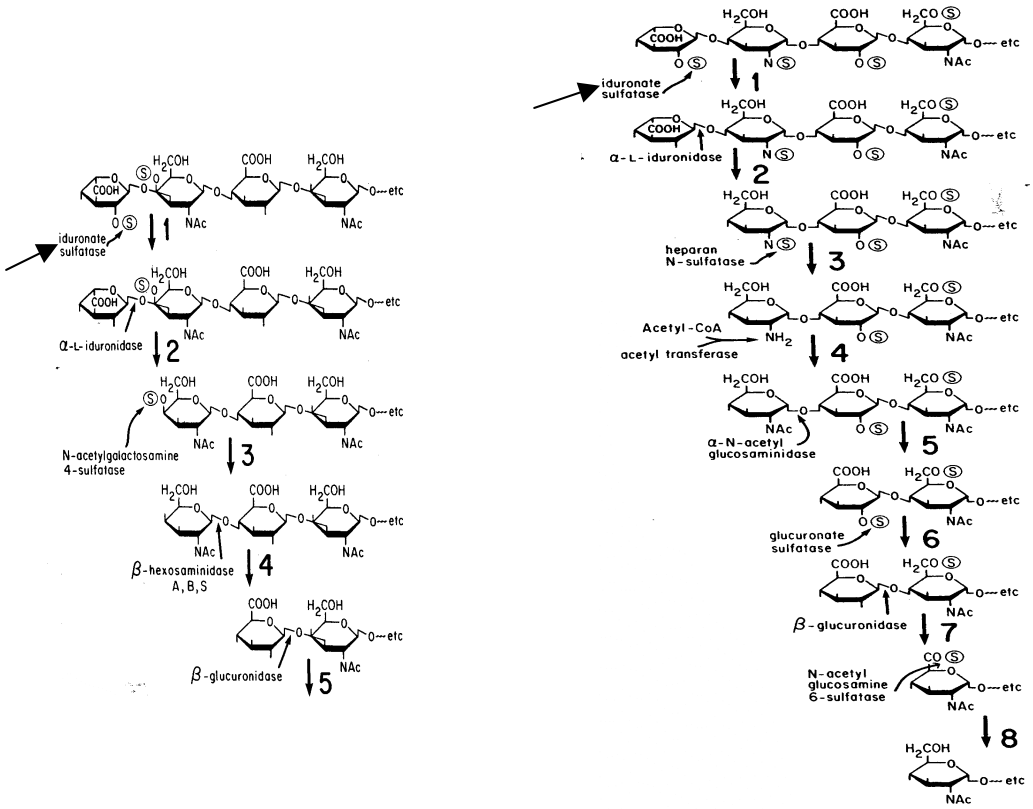

Figure 2(A-B): Catabolic process of dermatan (A: left of figure) and heparan sulfate (right of figure).

together. One of the parts of the extracellular matrix is a complex molecule called a proteoglycan. Like many components of the body, proteoglycans need to be broken down and replaced. When the body breaks down proteoglycans, one of the resulting products is mucopolysaccharides, otherwise known as GAG. There are several types of GAG, each found in certain characteristic places in the body. In Hunter syndrome, the problem concerns the breakdown of two GAG: dermatan sulfate and heparan sulfate. In people with Hunter syndrome, the IDS enzyme is either partially or completely inactive. As a result, GAG build up in cells throughout the body, particularly in tissues that contain large amounts of dermatan sulfate and heparan sulfate. As this buildup continues, it interferes with the way certain cells and organs in the body function and leads to

a number of serious symptoms. The rate of GAG buildup is not the same for all people with Hunter syndrome, resulting in a wide spectrum of medical problems.

- Children with MPS II A [28; 29] (Figure 3) are affected by coarse facial features, skeletal irregularities, obstructive airway and respiratory complications, short stature, joint stiffness, retinal degeneration (but no corneal clouding), communicating hydrocephalus [30], chronic diarrhea, enlarged liver and spleen, and progressive hearing loss. Whitish skin lesions may be found on the upper arms, back, and upper legs. Death from upper airway disease or cardiovascular failure usually occurs by age 15.

The symptoms of Hunter syndrome (MPS II) are generally not apparent at birth, but usually start to become noticeable after the first year of life. Often, the first symptoms of Hunter syndrome may include abdominal hernias, ear infections, runny noses, and colds. Since these symptoms are quite common among all infants, they are not likely to lead to make a diagnosis of Hunter syndrome right away. As the buildup of GAG continues throughout the cells of the body, signs of Hunter syndrome become more visible. Physical appearances of many children with Hunter syndrome include a distinctive coarseness in their facial features, including a prominent forehead, a nose with a flattened bridge, and an enlarged tongue. For this reason, unrelated children with Hunter syndrome often

look alike. They may also have a large head as well as an enlarged abdomen. Many continue to have frequent infections of the ears and respiratory tract. The continued storage of GAG in cells can lead to organs being affected in important ways. The thickening of the heart valves along with the walls of the heart can result in progressive decline in cardiac function. The walls of the airway may become thickened as well, leading to breathing problems while sleeping (obstructive airway disease). People with Hunter syndrome may also have limited lung capacity due to pulmonary involvement. As the liver and spleen grow larger with time, the belly may become distended, making hernias more noticeable. All major joints (including the wrists, elbows, shoulders, hips, and knees) may be affected by Hunter syndrome, leading to joint stiffness and limited motion. Progressive involvement of the finger and thumb joints results in decreased ability to pick up small objects. The effects on other joints, such as hips and knees, can make it increasingly difficult to walk normally. If carpal tunnel syndrome develops, a further decrease in hand function can occur. The bones themselves may be affected, resulting in short stature. In addition, pebbly, ivory-colored skin lesions may be found on the upper arms and legs and upper back of some people with Hunter syndrome. The presence or absence of the skin lesions is not helpful, however, in predicting clinical severity in Hunter syndrome. Finally, the storage of GAG in the brain can lead to delayed

development with subsequent mental retardation. The rate and degree of progression may be different for each person with Hunter syndrome.

- Physical characteristics of MPS II B [28; 29] (Figure 3) are less obvious and progress at a much slower rate. Diagnosis is often made in the second decade of life. Intellect and social development are not affected [29]. Skeletal problems may be less severe, but carpal tunnel syndrome and joint stiffness can restrict movement and height is somewhat less than normal. Other clinical symptoms include hearing loss, poor peripheral vision, diarrhea, and sleep apnea, although respiratory and cardiac complications can contribute to premature death. Persons with MPS II B may live into their 50s or beyond.

It is important to note that though the term mild is used by physicians in comparing people with Hunter syndrome, the effects of even mild disease are quite serious. Two of the most significant areas of variability concern the degree of mental retardation and expected lifespan. Some people who have Hunter syndrome are not mentally retarded and live into their 20s or 30s; there are occasional reports of people who have lived into their 50s or 60s. The quality of life remains high in a large number of people, and many adults are actively employed. In contrast, others with Hunter syndrome develop severe mental

impairment and have life expectation of 15 years or less. There are estimated to be approximately 2,000 people afflicted with Hunter Syndrome worldwide.

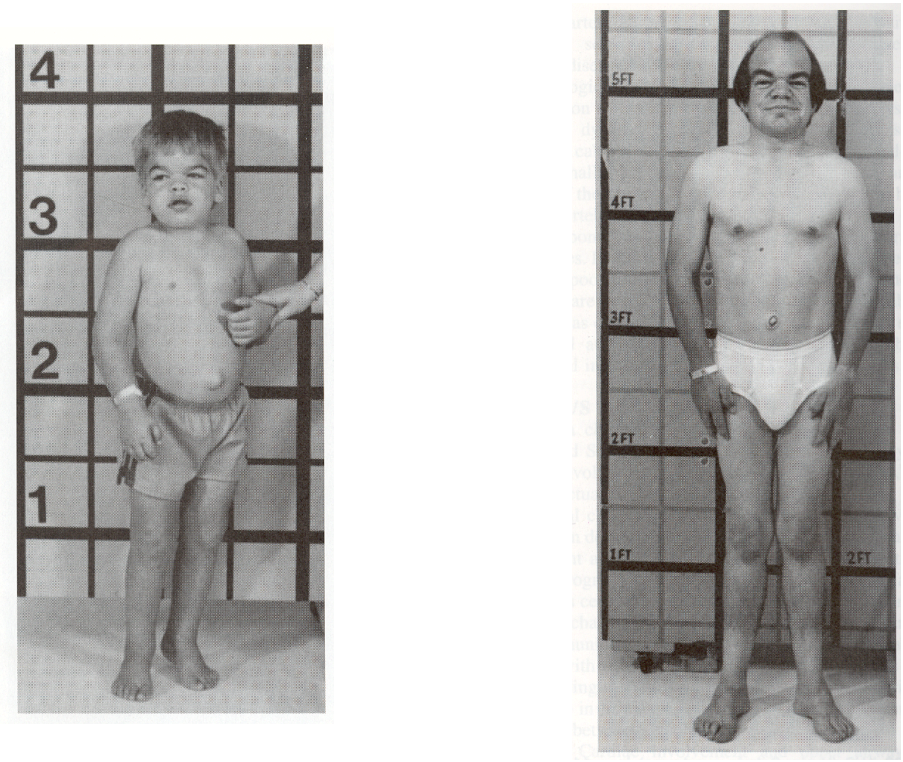

Figure 3(A-B): Patients affected by MPSIIA (A: left of figure) and by MPSIIB (B: right of figure).

6. MPSII KNOCK-OUT MOUSE MODEL

The MPSII mouse model (*Ids*$^{y/-}$) was generated by targeting exon 4 and part of exon 5 of the gene, and it has been characterized [31; 32].

7. THE GENE THERAPY

Gene therapy is the insertion of genes into an individual's cells and tissues to treat a disease, such as a hereditary disease in which a deleterious mutant allele is replaced with a functional one.

Germ line gene therapy

In the case of germ line gene therapy, germ cells, i.e., sperm or eggs, are modified by the introduction of functional genes, which are ordinarily integrated into their genomes. Therefore, the change due to therapy would be heritable and would be passed on to later generations. This new approach, theoretically, should be highly effective in counteracting genetic disorders and hereditary diseases. However, many jurisdictions prohibit this for application in human beings, at least for the present, for a variety of technical and ethical reasons.

Somatic gene therapy

In the case of somatic gene therapy, the therapeutic genes are transferred into the somatic cells of a patient. Any modifications and effects will be restricted to the individual patient only, and will not be inherited by the patient's offspring or later generations.

There are a variety of different methods to replace or repair the genes targeted in gene therapy. One of these is the replacement of gene using the viral vectors.

8. THE VIRAL VECTORS AND THE ADENO-ASSOCIATED VIRUSES (AAV)

All viruses bind to their hosts and introduce their genetic material into the host cell as part of their replication cycle. This genetic material contains basic instructions of how to produce more copies of these viruses, hijacking the body's normal production machinery to serve the needs of the virus. The host cell will carry out these instructions and produce additional copies of the virus, leading to more and more cells becoming infected. Some types of viruses physically insert their genes into the host's genome (a defining feature of retroviruses, the family of viruses that includes HIV, is that the virus will introduce the enzyme reverse transcriptase into the host and thus use its RNA as the instructions). This incorporates the genes of that virus among the genes of the host cell for the life span of that cell. The mechanism by which gene transfer occurs is the transduction [33]. Different kind of viral vectors can be used in the gene therapy protocols.

Retroviruses

The genetic material in retroviruses is in the form of RNA molecules, while the genetic material of their hosts is in the form of DNA. When a retrovirus infects a host cell, it will introduce its RNA together with some enzymes, namely reverse transcriptase and integrase, into the cell. This RNA molecule from the retrovirus

must produce a DNA copy from its RNA molecule before it can be integrated into the genetic material of the host cell. The process of producing a DNA copy from an RNA molecule is termed reverse transcription. It is carried out by one of the enzymes carried in the virus, called reverse transcriptase. After this DNA copy is produced and is free in the nucleus of the host cell, it must be incorporated into the genome of the host cell. That is, it must be inserted into the large DNA molecules in the cell (the chromosomes). This process is done by another enzyme carried in the virus called integrase. Now that the genetic material of the virus has been inserted, it can be said that the host cell has been modified to contain new genes. If this host cell divides later, its descendants will all contain the new genes. Sometimes the genes of the retrovirus do not express their information immediately. One of the problems of gene therapy using retroviruses is that the integrase enzyme can insert the genetic material of the virus into any arbitrary position in the genome of the host; it randomly shoves the genetic material into a chromosome. If genetic material happens to be inserted in the middle of one of the original genes of the host cell, this gene will be disrupted (insertional mutagenesis). If the gene happens to be one regulating cell division, uncontrolled cell division (i.e., cancer) can occur. This problem has recently begun to be addressed by utilizing zinc finger nucleases or by including certain sequences such as the beta-globin locus control region to direct the site of integration to specific chromosomal sites. Gene therapy trials using

retroviral vectors to treat X-linked severe combined immunodeficiency (X-SCID) represent the most successful application of gene therapy to date. More than twenty patients have been treated in France and Britain, with a high rate of immune system reconstitution observed. Similar trials were halted or restricted in the USA when leukemia was reported in patients treated in the French X-SCID gene therapy trial. To date, four children in the French trial and one in the British trial have developed leukemia as a result of insertional mutagenesis by the retroviral vector. All but one of these children responded well to conventional anti-leukemia treatment. Gene therapy trials to treat SCID due to deficiency of the Adenosine Deaminase (ADA) enzyme continue with relative success in the USA, Britain, Italy and Japan.

Adenoviruses

Adenoviruses are viruses that carry their genetic material in the form of double-stranded DNA. They cause respiratory, intestinal, and eye infections in humans (especially the common cold). When these viruses infect a host cell, they introduce their DNA molecule into the host. The genetic material of the adenoviruses is not incorporated (transient) into the host cell's genetic material. The DNA molecule is left free in the nucleus of the host cell, and the instructions in this extra DNA molecule are transcribed just like any other gene. The only difference is that these extra genes are not replicated when the cell is

about to undergo cell division so the descendants of that cell will not have the extra gene. As a result, treatment with the adenovirus will require readministration in a growing cell population although the absence of integration into the host cell's genome should prevent the type of cancer seen in the SCID trials. This vector system has been promoted for treating cancer and indeed the first gene therapy product to be licensed to treat cancer, Gendicine, is an adenovirus. Gendicine, an adenoviral p53-based gene therapy was approved by the Chinese FDA in 2003 for treatment of head and neck cancer. Concerns about the safety of adenovirus vectors were raised after the 1999 death of Jesse Gelsinger while participating in a gene therapy trial. Since then, work using adenovirus vectors has focused on genetically crippled versions of the virus.

Adeno-associated viruses

Adeno-associated viruses, from the parvovirus family [34], are small viruses with a genome of single stranded DNA. The major part of population is seropositive to the AAV [35; 36]. The wild type AAV can insert genetic material at a specific site on chromosome 19 with near 100% certainty [37; 38]. But the recombinant AAV, which does not contain any viral genes and only the therapeutic gene, does not integrate into the genome. Instead the recombinant viral genome fuses at its ends via the ITR (inverted terminal repeats) recombination to form circular, episomal forms which are predicted to be the primary cause of the long term gene

expression. There are a few disadvantages to using AAV, including the small amount of DNA it can carry (low capacity) and the difficulty in producing it. This type of virus is being used, however, because it is non-phatogenic (most people carry this harmless virus). In contrast to adenoviruses, most people treated with AAV will not build an immune response to remove the virus and the cells that have been successfully treated with it. Several trials with AAV are on-going or in preparation, mainly trying to treat muscle and eye diseases. However, clinical trials have also been initiated where AAV vectors are used to deliver genes to the brain. This is possible because AAV viruses can infect non-dividing (quiescent) cells [39], such as neurons in which their genomes are expressed for a long time.

MATERIALS AND METHODS

1. Animals

The female heterozygous MPSII mice were described [32].

2. Blood and tissue collection

Blood (50 µl) was collected in EDTA at different time points after the injection: T1, T6, T12, and T18 (until T12 for the *Ids*$^{y/-}$ control mice). The blood was centrifuged at 10,000x *g* for 10 min at 4 ˚C, and the serum (supernatant) was used for the enzyme assays. Tissues were collected 1 month and 18 months (14 months for the *Ids*$^{y/-}$ control mice) after injection. The mice were anaesthetized and sacrificed by cardiac perfusion: the left ventricle was cannulated, an incision was made in the right atrium, and the animals were perfused with PBS. The organs were collected. Half of each organ was fixed (for Alcian-blue and H&E staining, and IHC), and the other half was frozen in dry ice before being processed for the IDS activity assay and total RNA extraction.

3. AAV vector construction and production

The human IDS coding sequence was cloned into the pAAV2.1-CMV-LacZ plasmid[40] by replacing the LacZ sequence. The resulting pAAV2.1-CMV-hIDS and pAAV2.1-LacZ were then triple transfected in sub-confluent 293 cells, along with the pAd-Helper and the pack2/5 packaging plasmids, as described [41].

The recombinant AAV2/5 vectors were purified by two rounds of CsCl, as described [41]. Vector titers, expressed as genome copies (GC/ml), were assessed by real-time PCR (GeneAmp 7000 Applied Biosystem), as described [42]. The AAV vectors were produced by the TIGEM AAV Vector Core Facility.

4. IDS activity assay

The tissues for analysis were homogenized in water. Serum and tissue protein concentrations were determined using the Bio-Rad colorimetric assay (Bio-Rad, Hercules, CA, USA). The IDS assay was performed as described [43]: briefly, 50 µg total protein extract was incubated with 20 µl of the fluorogenic substrate, 4-methylumbelliferyl-α-iduronide-2-sulfate (Muscerdam Substrates), for 4 h at 37 ˚C. Then, 10 µl of purified α -iduronidase from rabbit liver (Muscerdam Substrates) and 40 µl of McIlvain's buffer (0.4 M Na-phosphate/ 0.2 M Na-citrate, pH 4.5) were added to the reaction mixture, which was then incubated for an additional 24 h at 37 ˚C. The reaction was stopped by adding carbonate stop buffer (0.5 M NaHCO3/0.5 M Na2CO3, pH 10.7), and the fluorescence of the 4-methylumbelliferone liberated was measured using 365 nm excitation and 460 nm emission in a fluorimeter (BIO-RAD VersaFluor Fluorometer). The enzyme activities were expressed as nmol/4 h/mg protein, as calculated through the standard curve of the fluorogenic substrate, 4-methylumbelliferyl-α-iduronide (Sigma-Aldrich).

5. Alcian blue and H&E staining

After the perfusion of the animals with PBS, the tissues were collected and fixed in methacarn solution (30% chloroform, 60% methanol and 10% acetic acid) for 24 h at 4 ˚C. The next day, the tissues were embedded in paraffin (Sigma-Aldrich) after their dehydration with a 70% to 100% ethanol gradient. Finally, the tissues were sectioned into 7-µm-thick serial sections. The tissue sections were stained with 1% Alcian blue (Sigma-Aldrich) in hydrochloric acid. The counterstaining was performed for 2 min with Nuclear-Fast red (Sigma-Aldrich). For the H&E staining, the brains were collected after PBS perfusion and fixed in methacarn solution, embedded in paraffin, sectioned into 7-µm-thick sections, and then stained with Hematoxylin (Sigma-Aldrich) for 2 min. The counterstaining was performed with Eosin (Sigma-Aldrich) for 30 s.

6. Immunohistochemistry

Mice brains were collected after PBS perfusion and fixed with 10% neutral buffered formalin (NBF), pH 7.0, for 12 h at 4 ˚C. Then the brains were embedded in paraffin (Sigma-Aldrich), and then dehydrated with a 70% to 100% ethanol gradient. Immunohistochemistry analyses were performed on 7-µm-thick serial sections. The specimens were incubated for 1 h with blocking solution (Tris-buffered saline, 0.2% Tween-20 [Sigma-Aldrich], and 10%

normal horse serum, Vectastain Elite ABC kit) before incubation overnight with the primary antibodies.

For immunohistochemical analysis of NeuN, ubiquitin, GFAP and α-synuclein of the paraffin-embedded, formalin-fixed brains, the avidin-biotin complex (ABC) method was used (Vectastain Elite ABC kit). Monoclonal rabbit antibodies against murine NeuN (diluted 1:100; Chemicon International), ubiquitin (polyclonal; diluted 1:50; Abcam, Cambridge, UK), GFAP (diluted 1:200; Sigma-Aldrich) and α-synuclein (diluted 1:250; Abcam, Cambridge, UK) antibodies were used. For detection of CD68, a monoclonal rat antibody against murine CD68 was used (diluted 1:250; AbD Serotec). Then a secondary biotinylated horse anti-rabbit IgG and streptavidin-biotin-peroxidase complex (Vectastain Elite ABC kit) were used for 1 h of incubation (for anti-NeuN, ubiquitin, GFAP, α-synuclein). For anti-CD68 secondary biotinylated horse anti-rat IgG was used (Vector Laboratories, CA, USA). The colour was developed using the ABC Elite Vector Staining kit and the horseradish peroxidase substrate (Vector Laboratories, Inc., Burlingame, CA). For the detection of apoptotic cells in the brain sections, we used the TUNEL staining kit (Chemicon International), according to the manufacturer instructions.

7. RT-PCR

RNA was extracted from the brains, livers and lungs of wt, *Ids*$^{y/-}$ and injected *Ids*$^{y/-}$ mice sacrificed 1 month and 18 months after treatment. The cDNAs were obtained by Superscript III Reverse Transcriptase kits (Invitrogen). The primers used were: forward primer hIDS: 5'-cagcagcgagaagtacgaga-3'; reverse primer hIDS: 5'-ttctggaactccttggggta-3'; forward primer mIDS: 5'-tccaccttatcatccatcct-3'; reverse primer mIDS: 5'-gccagggttatgttttccaa-3'; forward primer LacZ: 5'-actatcccgaccgccttact-3'; reverse primer LacZ: 5'- tagcggctgatgttgaactg-3'; forward primer mGAPDH: 5'-gtcggtgtgaacggatttg-3'; and reverse primer mGAPDH: 5'-caatgaaggggtcgttgatg-3'. The amplicon sizes were, respectively, 241, 285, 173 and 100 bp. Each reaction was carried out using 300 ng of sample cDNA in a final volume of 25 μl (with EuroTaq-Euroclone). The following cycling parameters were used: 5 min at 94 °C, followed by 33 cycles of denaturation at 94 °C for 1 min, annealing at 59 °C for 1 min (for hIDS and LacZ), or at 56 °C for 1 min (for mIDS and mGAPDH), extension at 72 °C for 1 min, followed by 7 min at 72 °C.

8. Quantitative real-time PCR

Real-time PCR was performed on genomic DNA extracted from the brain and liver of the injected mice 1 month after treatment (on a LightCycler 480 Probes Master Roche machinery). The primers used were: forward primer BGH: 5'-

tctagttgccagccatctgttgt-3'; reverse primer BGH: 5'-tgggagtggcaccttcca-3' and the TaqMan probe 5'-6FAM-tcccccgtgccttccttgacc-TAMRA-3'. Amplicon size was 65 bp. Each reaction was carried out using 100 ng of sample genomic DNA in a final volume of 25 μl (with LightCycler 480 Probes Master kit, Roche). As standard, the diluted gene transfer vector was used (from 1×10^7 copies to 1 copy/reaction). The following cycling parameters were used: 5 min at 95 °C, followed by 45 cycles of denaturation at 95 °C for 10 sec, annealing at 60 °C for 35 sec, extension at 72 °C for 1 sec, followed by 10 sec at 40 °C.

All the reactions were performed in triplicate sets and the results were reported as the average of three reactions.

To obtain the vector copy number for each cell, the values were divided by the number of cells corresponding to 100 ng of genomic mouse DNA.

9. Quantitative analysis of GAG accumulation in the urine

Urine from individual mice was collected in metabolic cages at different times during the treatment: T1, T6, T12 and T18 (until T12 for the *Ids*$^{y/-}$ control mice). The GAG levels in the urine were determined using the dimethylmethylene blue-based spectrophotometry of GAGs [44]. These were normalized to the creatinine content. Urine creatinine was measured using a Creatinine Assay kit (Quidel Corporation, San Diego, CA, USA). Absorbance was read at 490 nm. The urinary GAG was expressed as mg GAG/mg creatinine.

10. Open-field test

Treated *Ids*$^{y/-}$+IDS (T18) and control mice (wt, *Ids*$^{y/-}$) were tested during the same sessions to minimize any variability. The motor and the exploratory behaviours were assessed in an acrylic open arena, as described [45].

11. Statistical analyses

It was measured the statistical significance of compared measurements with the Student's two-tailed t-test.

RESULTS

1. Knock-out mouse model of Hunter syndrome

MPSII is an X-linked recessive lysosomal storage disorder that is caused by the lack of IDS activity. Iduronate-2-sulfatase (IDS) is the enzyme that removes the sulfate group from dermatan and heparan sulfate, and its inactivity results in MPSII, or Hunter syndrome, a rare X-linked inborn error of metabolism.

Usually, only males are affected. The incidence of MPSII has been estimated at around 1 in 162,000 live births. The deficiency of IDS has been shown to be due to point mutations or deletions in the 24 kb IDS gene [26]. As with all of the human sulfatases, IDS needs to be activated by sulfatase modifying factor 1 (SUMF1) [24; 25].

MPSII occurs in both severe and mild forms that cover a broad spectrum of symptoms with slow to rapid pathological progression. The severe form is characterized by progressive somatic and neurological involvement, with an onset between the second and fourth years of age and an early mortality. Facial features, hepatosplenomegaly, short stature, skeletal deformities, joint stiffness, severe retinal degeneration, and hearing impairment are coupled to an incremental deterioration of the neurological system [27]. We and others always described the phenotype of the knock-out mouse model (*Ids*$^{y/-}$) of MPSII [31; 32].

The MPSII (*Ids*$^{y/-}$) mouse model displays the features of Hunter syndrome [31]. We observed that the onset of the gross morphological phenotype was clearly

manifested at 3–4 months of age, and it became progressively severe through their adult life; the affected mice usually died by 60–70 weeks of age. This phenotype includes craniofacial abnormalities, with a short cranium and alopecia; thickening of the digits was also seen. Furthermore, the older MPSII mice weighed less than each matched wild-type animal. The protein extracts prepared from tissue homogenates of the MPSII mice were tested for IDS activity using the fluorescent substrate 4-methylumbelliferyl-a-iduronate 2-sulfate [31]. IDS activity was undetectable in liver, spleen, lung, heart, kidney, skeletal muscle, brain and eye when compared with the activities of this enzyme in the wild-type tissues [32].

IDS initiates the catabolism of the dermatan and heparan sulfate GAGs. The loss of IDS activity causes GAG accumulation within the urine and all tissues, with a progressive cellular vacuolization and the consequent cell death. We thus analyzed GAG accumulation in the early stages of the affected mice: at 1 day of age (p1) and at 3 days of age (p3). GAG accumulation was already detectable in the tissues at these early stages of life [32]. GAG accumulation dramatically increased during the adult stages, and Alcian-blue staining of the paraffin-embedded sections of liver, spleen, lung, heart, kidney and skeletal muscle of *Ids*$^{y/-}$ mice at 3 and 9 months of age showed high levels of GAG storage within the cells [32]. This progressive increase in GAG lysosomal storage also caused skeleton deformation. In particular, a craniofacial abnormality was evident,

which was characterized by a longer length between the base of the ears and a shorter distance across the maxilla and the zygoma [32]. The skeleton malformations also affected the performance in locomotor tests. Indeed, the MPSII mice showed irregular gait, abnormal walking pattern and poor locomotor and exploratory abilities in the open-field test [32].

In addition, we observed that MPSII mice presented neuropathological defects [32].

2. IDS gene delivery in the MPSII mice

MPSII is characterized by the involvement of many visceral organs, including the heart, kidney, liver, lung, muscle, spleen and brain. Previously, we used an AAV type 2/8 vector carrying human IDS cDNA under the control of the thyroxine-binding globulin liver-specific promoter (AAV2/8TBG-hIDS), to engineer liver secretion of IDS.

We shown that systemic administration of AAV2/8TBG-hIDS can lead to very high levels of circulating IDS, which efficiently corrected the visceral organs through IDS uptake from the blood [32] and partially cleared glycosaminoglycan (GAG) accumulation in the choroid plexus of *Ids*$^{y/-}$ mice [32]. We used the human IDS gene transfer to engineer the liver to secrete the active sulfatase into the blood stream at sufficiently high levels to systemic cross-correct the enzymatic deficiencies in the various tissues. We constructed an AAV type 2/8 vector

carrying the human IDS cDNA under the transcriptional control of the liver-specific promoter of the TBG gene (AAV2/8TBG-IDS) [40]; adult MPSII mice received 1.0 x 10^{11} particles of AAV2/8TBG-IDS in a volume of 200 ml via the tail vein [32].

It was imperative to develop an efficient therapy to treat the CNS symptoms. Ideally, having circulating IDS that crosses the blood-brain barrier (BBB) would be highly preferred and would provide treatment of both visceral and CNS defects, simultaneously.

The BBB is formed by a layer of endothelial cells of the brain microvasculature that regulates the passage of molecules between the blood and the CNS. Tight junctions block the passage of most molecules, except some specific substances that cross the BBB via receptor-mediated transport [46] (Figure 4).

Enzyme-replacement therapy at high doses in mouse models of α-mannosidosis, MPSVII, and metachromatic leukodystrophy leads to enzyme delivery across the BBB, thereby partially reversing storage in brain tissues [47-49]. Similarly, the intrahepatic administration of AAV2 vectors in MPSVII mice results in some correction of the CNS phenotype [50].

To anticipate disease manifestation and to simultaneously treat the visceral and CNS defects of MPSII, we have been systemically administered the AAV type 2/5 vector carrying human IDS cDNA, but here under the control of the

cytomegalovirus promoter (AAV2/5CMV-hIDS), in day 2 (p2) *Ids*$^{y/-}$ mouse pups.

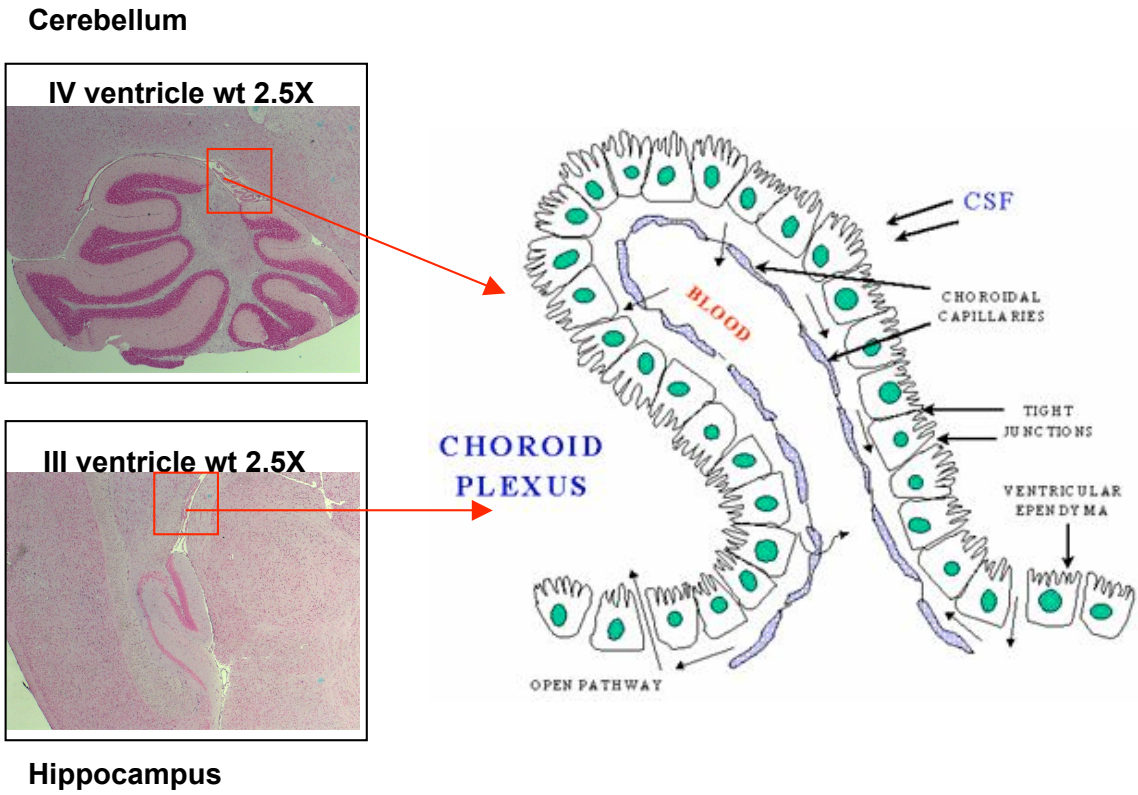

Figure 4. General structure of Blood-Brain Barrier (BBB).

We used this type of vector because it has been shown to provide efficient transduction of several tissues, such as skeletal muscle and lung [51; 52].

We injected groups of p2 *Ids*$^{y/-}$ pups in the temporal vein with 1 x 10^{11} AAV2/5CMV-hIDS viral particles; along with a group of non-injected MPSII (n = 5) and of wild-type (n = 5) mice, these mice were all then analyzed in the following ways:

(1) The mice under the therapeutic protocol were checked every 6 months for 18 months for IDS activity in their plasma and for the GAG content of their urine.

(2) The mice were sacrificed at two times after transduction: one group of injected mice (T1; n = 8) after 1 month and the other group of injected mice (T18; n = 4) at 18 month of therapy. In parallel, groups of untreated *Ids*$^{y/-}$ and wild-type control mice of the same age were sacrificed as controls. We analyzed all tissues of the sacrificed mice for IDS activity and GAG clearance.

We observed full correction of the CNS symptoms and visceral defects. Furthermore, we provided evidence that correction of CNS storage and neuronal markers is due to the crossing of the BBB by IDS.

3. Rescue of the IDS activity in the tissues and in the brain of adult MPSII mice by AAV2/5CMV-hIDS

The data collected on the MPSII mice tissues and plasma at T1, T6, T12 and T18 are reported. The plasma IDS activity that we monitored every 6 months for 18 months was extremely high, showing levels up to 5-fold higher in the treated mice in comparison to the WT mice and up to 60-fold higher in the treated mice in comparison to the *Ids*$^{y/-}$ control mice (Table 1). The untreated *Ids*$^{y/-}$ mice died at 14 months. In contrast, the life span of the treated animals was prolonged up to and beyond 18 months.

On average, the levels were always much higher than the wild-type activity throughout the period of the treatment, although there was a decrease in plasma IDS activity during the therapy. This fall of IDS activity might be due to a loss over time of viral DNA copies or to a slight immune response toward the transgene or toward the AAV capsid. The IDS plasma activity in untreated mice (Table 1) was not detectable.

We sacrificed eight treated MPSII mice at T1 and four at T18 after gene delivery. As the control, two groups of five untreated and wild-type mice of comparable ages were sacrificed.

We determined the IDS activities in protein extracts prepared from the homogenized tissues of all the control and treated mice. In the treated mice, there was a remarkable rescue of IDS activity that reached levels comparable to or higher than the IDS activities measured in the WT tissues; this was seen for all of the evaluated tissues from the treated mice that were sacrificed at T1 and T18. As expected, in the tissues of the untreated MPSII, the IDS activity was not detectable (Figure 5A).

Surprisingly, a moderate rescue of IDS activity was evident in brain homogenates of T1 and T18 mice (Figure 5B).

Table 1. IDS Activity in the Plasma

	IDS Activity (nmol/4 h/mg)			
	T1	**T6**	**T12**	**T18**
WT	320 ± 27	243 ± 32.1	220 ± 36.2	198 ± 18.9
Ids$^{y/}$	27 ± 1.5	24 ± 0.6	18 ± 1.1	
Ids$^{y/}$ +IDS	2400			
Ids$^{y/}$ +IDS	2700			
Ids$^{y/}$ +IDS	1995			
Ids$^{y/}$ +IDS	2090			
Ids$^{y/}$ +IDS	2405			
Ids$^{y/}$ +IDS	2820			
Ids$^{y/}$ +IDS	1900			
Ids$^{y/}$ +IDS	2340			
Ids$^{y/}$ +IDS	2300	1410	909	820
Ids$^{y/}$ +IDS	1900	950	659	420
Ids$^{y/}$ +IDS	2435	1680	1409	1219
Ids$^{y/}$ +IDS	2230	1735	1380	1022

Table 1. IDS activity in the plasma measured at different times after therapy (T1, T6, T12, and T18: 1, 6, 12, and 18 months after the injection, respectively) of WT (n = 3), *Ids*$^{y/-}$ (n = 3), and AAV2/5CMV-hIDS-injected *Ids*$^{y/-}$ mice.

Altogether, these results demonstrate that the systemic injection of the AAV2/5CMV-hIDS viral particles results in an extremely efficient production, secretion and uptake of the IDS enzyme.

Moreover these results led to predict that IDS enzyme had crossed the BBB. Indeed, much higher IDS activity would be expected if there had been transduction of AAV2/5CMV-hIDS in the brain.

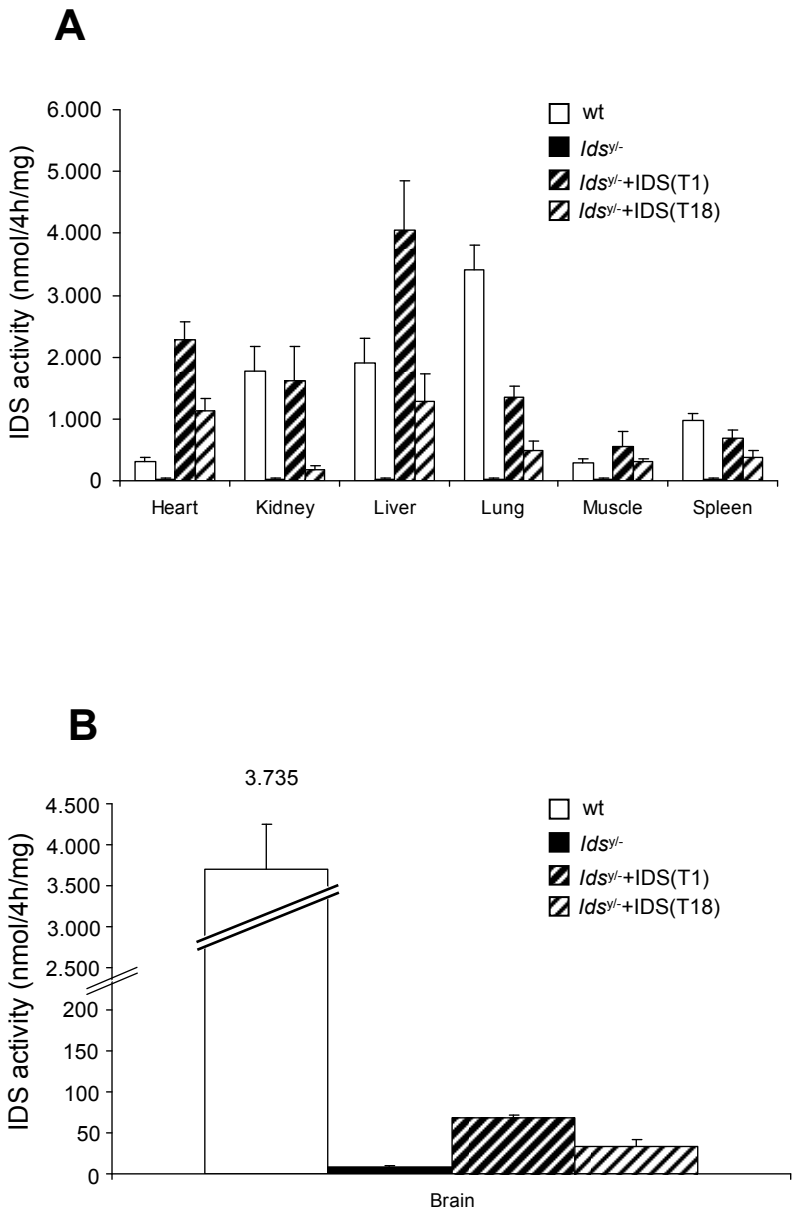

Figure 5. Increase in IDS Activity and Rescue of GAG Accumulation in *Ids*$^{y/-}$ Mice after Temporal Vein AAV2/5CMV-hIDS Injection

(A) P2 *Ids*$^{y/-}$ mice sacrificed 1 (T1) and 18 (T18) months after therapy. IDS activities in the treated mice were measured in protein extracts of: WT (n = 5), *Ids*$^{y/-}$ (n = 5), T1 *Ids*$^{y/-}$+IDS (n = 8), and T18 *Ids*$^{y/-}$+IDS (n = 4) mice. **(B)** IDS measured in brain homogenates of the same groups of control and treated mice. Error bars indicate standard deviations. $p < 0.05$ (Student's t test).

4. Clearance of the lysosomal GAG accumulation in the tissues and in the urine of treated MPSII mice

To determine whether the IDS activity mediated by AAV2/5CMV-hIDS was able to clear the GAG lysosomal storage of the MPSII mice, we measured the GAG content in the tissues and in the urine of control and treated mice.

The urine of the treated MPSII (T1, n = 8; T18, n = 4), untreated (n = 3) and wild-type (n = 3) mice were analyzed for their GAG levels every 6 months for up to 18 months after the injections at T1, T6, T12, and T18.

The GAG levels were normalized with respect to the urine creatinine content (GAG excretion is expressed as a ratio of milligrams of GAGs to milligrams of creatinine excretion). The GAG accumulation in the urine of the MPSII mice was approximately double the concentration found in the wild-type animals. GAGs were cleared in the urine of all of the treated mice for up to 18 months after the therapy, and their accumulation was almost fully normalized, as compared to WT levels (Table 2).

For the tissues, we evaluated the GAG lysosomal storage using quantitative Alcian-blue staining. At T1 and T18, the organs of the sacrificed treated MPSII mice (T1, n = 8; T18, n = 4) were embedded in paraffin and the GAG accumulation analyzed in sections.

As expected, the GAG lysosomal storage in the control, untreated MPSII tissues was highly positive in the Alcian-blue staining.

	GAG Accumulation (mg GAG/mg creatinine)			
	T1	T6	T12	T18
wt	16.0 ±0.6	17.0 ±1.0	19.0 ±1.0	19.0 ±1.1
Ids$^{y/-}$	34.0 ±1.1	47.0 ±2.0	51.0 ±1.2	
Ids$^{y/-}$+IDS	22.0			
Ids$^{y/-}$+IDS	21.5			
Ids$^{y/-}$+IDS	22.3			
Ids$^{y/-}$+IDS	24.0			
Ids$^{y/-}$+IDS	23.0			
Ids$^{y/-}$+IDS	24.4			
Ids$^{y/-}$+IDS	21.0			
Ids$^{y/-}$+IDS	22.8			
Ids$^{y/-}$+IDS	21.0	22.5	22.0	25.0
Ids$^{y/-}$+IDS	22.0	24.0	27.0	28.0
Ids$^{y/-}$+IDS	24.0	25.1	23.0	29.0
Ids$^{y/-}$+IDS	23.2	24.5	24.0	26.0

Table 2. GAG accumulation in the urine measured at different times after therapy (T1-T6-T12-T18) (1-6-12-18 months after the injection, respectively) of wt (n = 3), *Ids*$^{y/-}$ (n = 3) and *Ids*$^{y/-}$ AAV2/5CMV-hIDS-injected mice. $P<0.05$ (Student's *t*-test). GAG concentrations were normalized against urine creatinine contents.

GAG accumulation was fully cleared in the visceral tissues of both of these treated groups (T1 and T18) (Figure 6).

These data show that by using AAV2/5CMV-hIDS-mediated gene delivery, we were able to correct the metabolic disorder for up to 18 months of treatment.

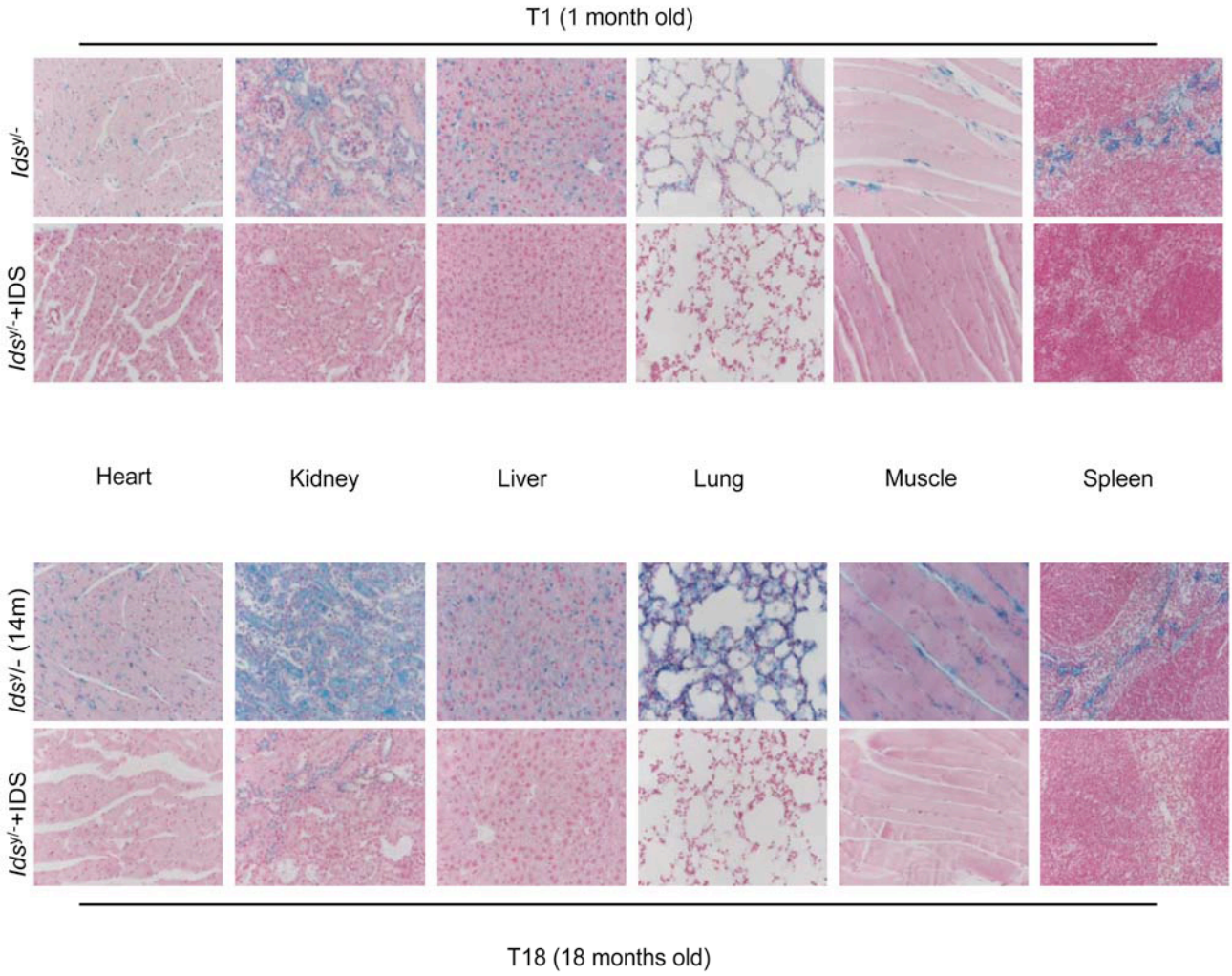

Figure 6. Clearance of GAG Accumulation in all Tissues of *Ids*$^{y/-}$+IDS (T1) and *Ids*$^{y/-}$ +IDS (T18) Injected Mice

Qualitative GAG accumulation measured by Alcian Blue staining of sections of all tissues of *Ids*$^{y/-}$ (T1-T14) and *Ids*$^{y/-}$+IDS (T1-T18) mice. Magnification, 20x.

5. Characterization and complete correction of the brain defects in the treated MPSII mice

The severe form of MPSII (MPSIIA) in human is characterized by mental retardation, cervical cord compression and foramen magnum stenosis, possibly leading to hydrocephalus [4]. We analyzed the MPSII mice to check for the presence of neuropathological features within the CNS [32].

The IDS activity that we measured in brain homogenates of MPSII mice was not detectable [32]. Histopathological examination of brain sections were performed on MPSII mice at 4 months after birth by Toluidine-blue staining. Cellular vacuolization was detected in different regions of the brain in all of the *Ids*$^{y/-}$ mice examined: the hippocampus, thalamus, cerebellum and brainstem. In the cerebellum, reduced numbers and atypical morphology of the Purkinje cells were observed [32], probably due to the accumulation of GAGs, with consequent cell vacuolization and death. Finally, we evaluated GAG accumulation through Alcian-blue staining of the brain sections. GAG accumulation was detected within the choroid plexus of the ventricular region.

Interestingly, we seen clearly diffuse neurodegeneration in the thalamus, cerebral cortex, and brainstem of untreated animals, through observation of reduced neuronal density (decreased anti-NeuN signal) and increased ubiquitin-expressing neurons, as compared to the WT brain areas. This was also associated with the triggering of apoptosis, as shown by TUNEL positive signals

in neurons of the thalamus, cerebral cortex, and brainstem of MPSII mice (Figure 7A and Figures 8 and 9). In addition, in the white matter, there were α-synuclein aggregates (Figure 4B), which have previously been shown to accumulate in neurons during neurodegenerative disorders, such as Parkinson disease and Alzheimer disease, and also during lysosomal storage disorders, such as Sandhoff disease, Tay-Sachs disease, metachromatic leukodystrophy, and β-galactosialidosis [53].

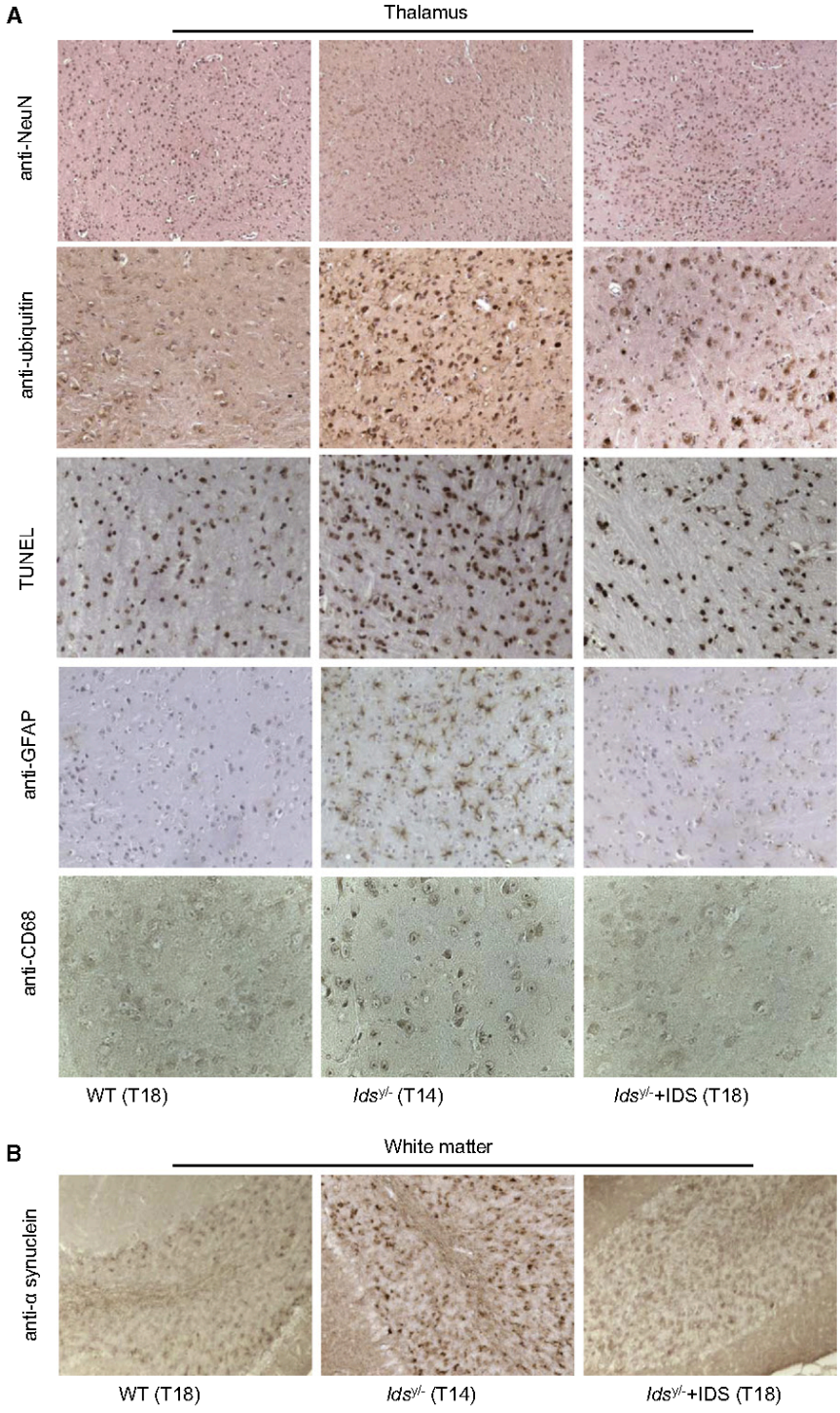

Figure 7. Rescue of Brain Defects in AAV2/5CMV-hIDS-Injected *Ids*$^{y/-}$ Mice
(A and B) Immunohistochemistry of different brain-specific markers (monoclonal anti-NeuN, diluted 1:100; polyclonal anti-ubiquitin, diluted 1:50; TUNEL; monoclonal anti-GFAP, diluted 1:200; and monoclonal anti-CD68, diluted 1:250) in the thalamus and white matter (monoclonal anti-α-synuclein, diluted 1:250) of brain sections in T18 WT, T14 *Ids*$^{y/-}$, and T18 AAV2/5CMV-hIDS-injected *Ids*$^{y/-}$ mice. Magnification: 10x (anti-NeuN sections); 40x (anti-CD68 sections); or 20x (all others).

Finally, in the untreated mice, there we found also increased numbers of activated microglia (GFAP immunohistochemistry) and massive infiltration of activated macrophages (CD68 positivity) (Figure 7A and Figures 8 and 9).

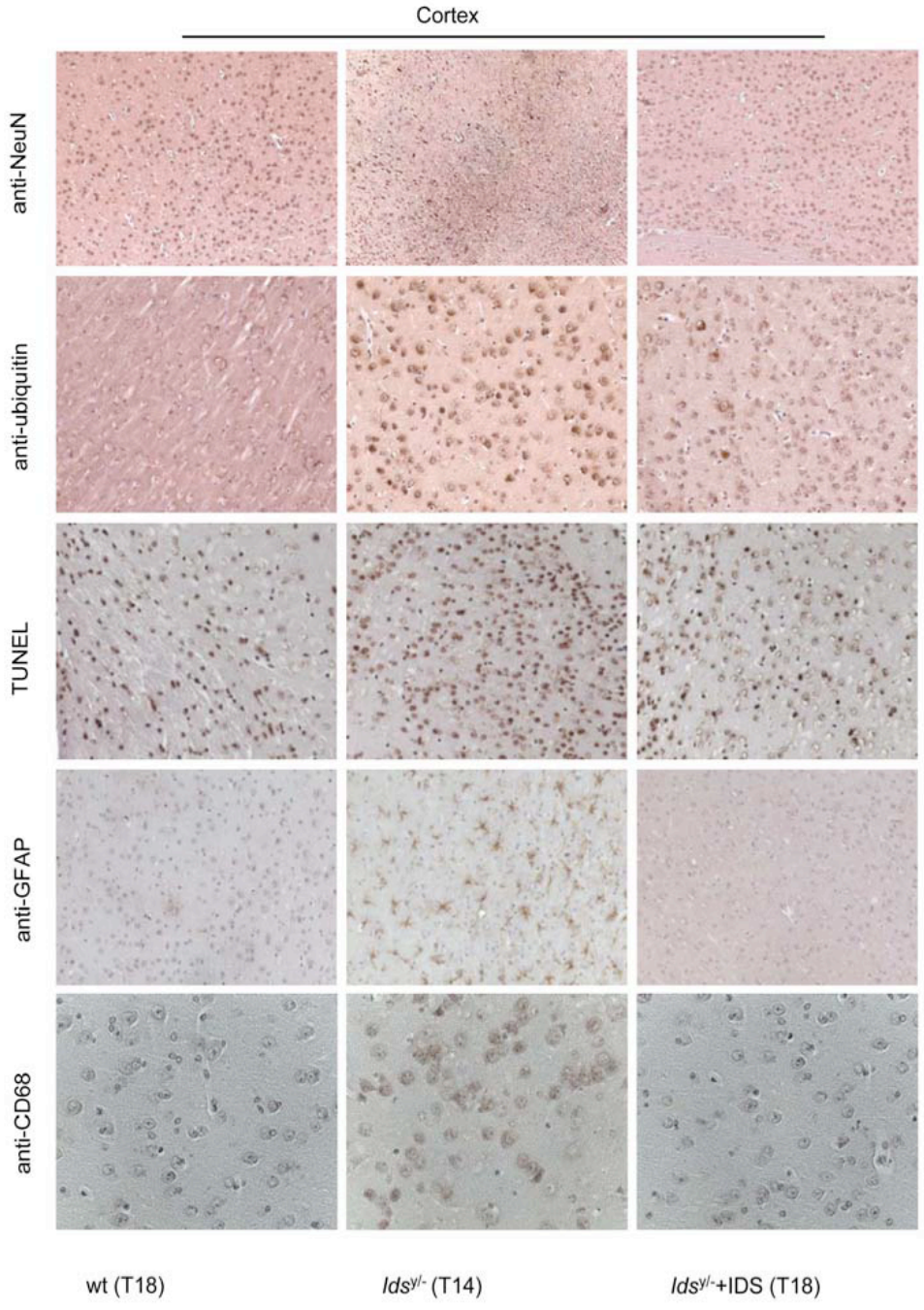

Figure 8. Rescue of Brain Defects in *Ids*$^{y/-}$ Treated Mice
Immunohistochemistry of different specific brain markers (anti-NeuN, anti-ubiquitin, TUNEL, anti-GFAP and anti-CD68) in cortex of wt (T18), *Ids*$^{y/-}$ (T14), *Ids*$^{y/-}$+IDS (T18) brains. Magnification, 10x (anti-NeuN sections); 40x (anti-CD68 sections); 20x (all others).

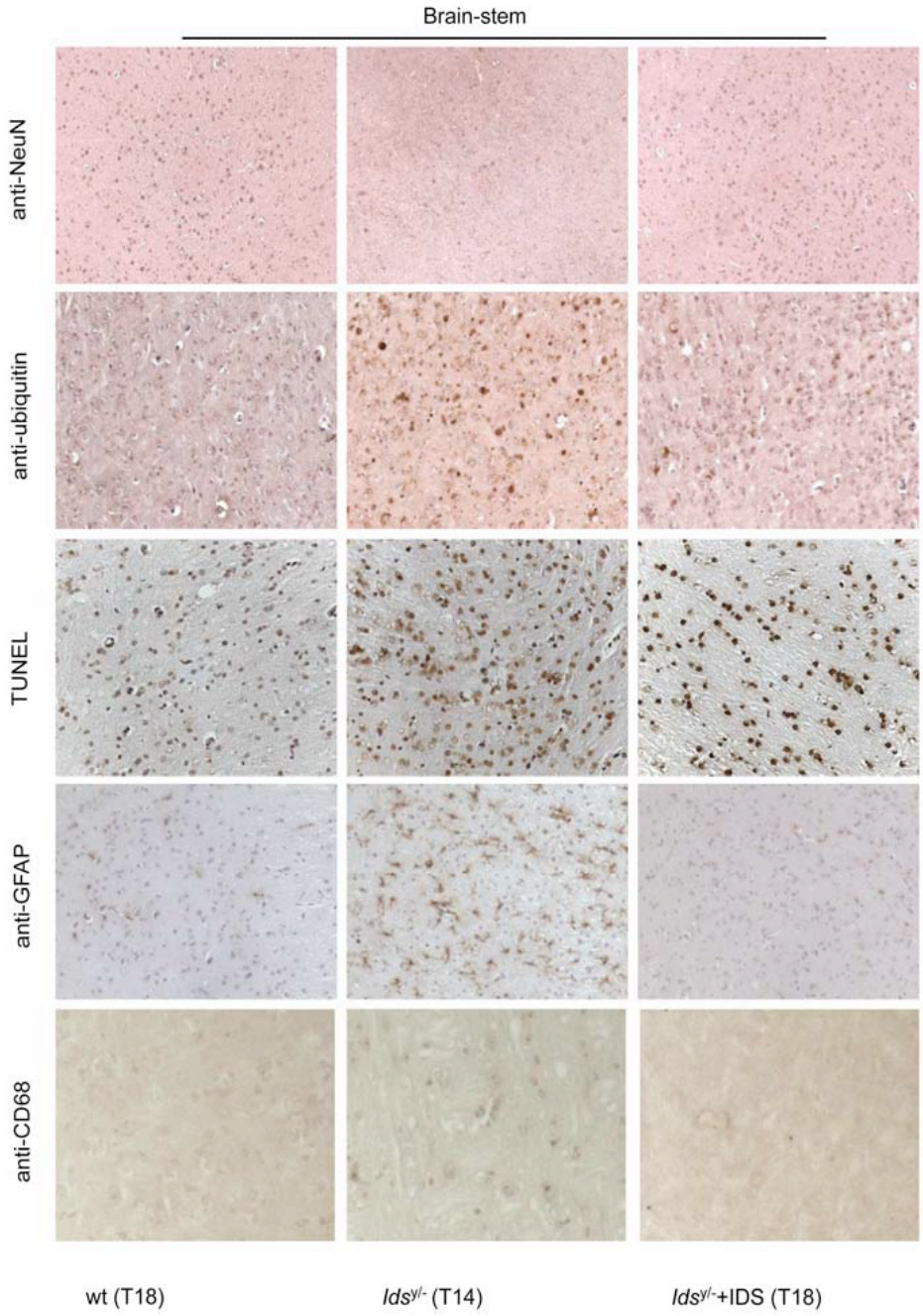

Figure 9. Rescue of Brain Defects in *Ids*$^{y/-}$ Treated Mice
Immunohistochemistry of different specific brain markers (anti-NeuN, anti-ubiquitin, TUNEL, anti-GFAP and anti-CD68) in brain stem of wt (T18), *Ids*$^{y/-}$ (T14), *Ids*$^{y/-}$+IDS (T18) brains. Magnification, 10x (anti-NeuN sections); 40x (anti-CD68 sections); 20x (all others).

In our previous work, the GAG accumulation was already partially rescued in the choroid plexus of IV ventricle in the treated adult MPSII mice, with AAV2/8 serotype [32]. This was surprising, given the presence of the hematoencephalic barrier. We predicted that because of the very high levels of IDS in the plasma, which ranged from 16- to 70-fold higher than the normal wild-type values, a fractional amount of the enzyme crosses the barrier and corrects the defect. To further confirm this result, we performed immunohistochemistry experiments. A group of MPSII mice were injected with 4.0 x 10^{12} AAV2/8TBG-IDS particles and sacrificed 1 month after the therapy. The brains and the livers of the injected mice and of non-injected and wild-type animals were included in OCT and the tissue sections were hybridized with an anti-hIDS polyclonal serum. This antibody recognizes only the human protein, and not the mouse form. The brain sections were also co-stained with an anti-Lamp2 monoclonal antibody, as a lysosomal marker. Positive lysosomal signals were detected in the brain and specifically in the cortex and cerebellum of the injected MPSII mice [32]. A positive signal was also detected in the liver sections, as expected. No signal was present in the lysosomes of brains of wild-type or MPSII mice [32].

To anticipate the disease manifestations and to obtain a therapeutic effect in the CNS, we systemically injected MPSII pups (p2) with 1.0 x 10^{11} AAV2/5CMV-hIDS particles in the temporal vein.

The progressive accumulation of GAGs in lysosomes of neurons leads to severe GAG accumulation and vacuolization. This was cleared in neurons of the brainstem, cortex, hippocampus, and thalamus of treated mice. We confirmed the reduced cellular vacuolization by hematoxylin and eosin staining (Figure 10).

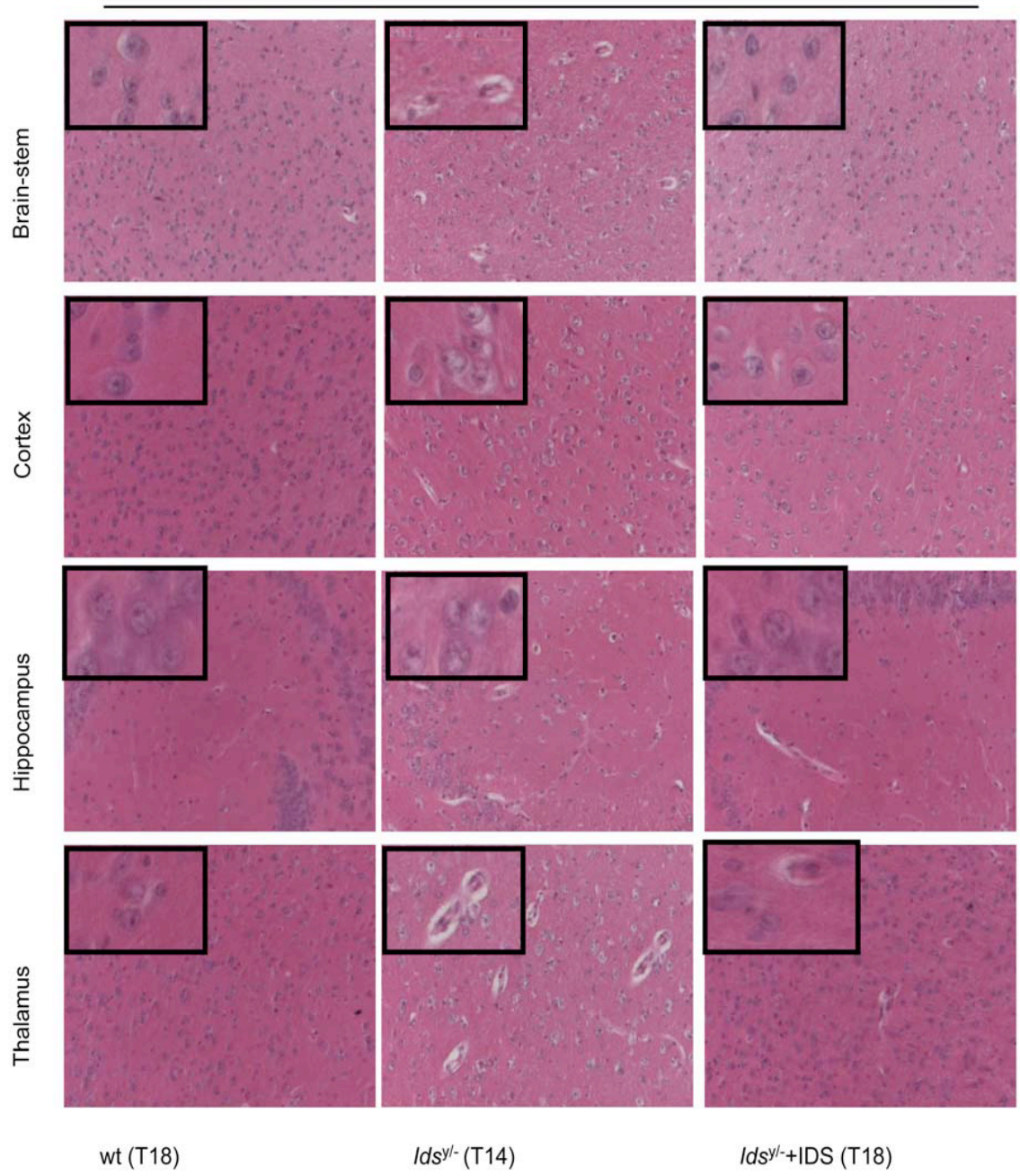

Figure 10. Clearance of Vacuolization in Brain Sections of Treated Mice
H&E stained sections of different regions of brains of wt (T18), *Ids*$^{y/-}$ (T14) and *Ids*$^{y/-}$+IDS (T18) mice. Magnification, 20x (black box, 40x).

GAG accumulation, by Alcian-blue staining, was fully cleared for both treated groups (T1, T18), remarkably, in all of the brain areas analyzed: the choroid

plexus in the IV and III ventricles, as well as the meninges, brainstem, cortex, hippocampus, and thalamus (Figure 11A and Figure 11B).

Remarkably, in the T18 AAV2/5CMV-hIDS-injected *Ids*$^{y/-}$ mice, we found clear amelioration or complete correction of neurodegeneration (normalized staining of NeuN, ubiquitin, TUNEL, and α-synuclein), astrogliosis (normalized GFAP staining), and inflammation (normalized CD68 staining) (Figures 7A and 7B and Figures 8 and 9). Furthermore, in one-month-old MPSII mice, we observed increases in ubiquitin-expressing neurons and astroglysosis in the thalamus, including an increase in α-synuclein aggregates as well; these markers were normalized in the group of T1 AAV2/5CMV-hIDS-injected *Ids*$^{y/-}$ mice (Figures 12A and 12B).

All of these data demonstrate that with this therapy, it's possible to prevent the development of the CNS defects, along with the somatic manifestations.

These data clearly showed that, even if only a partial rescue of the IDS activity in the brain was succeeded with this therapy, this constant low level of IDS that had crossed the BBB was sufficient to totally clear the GAG CNS storage.

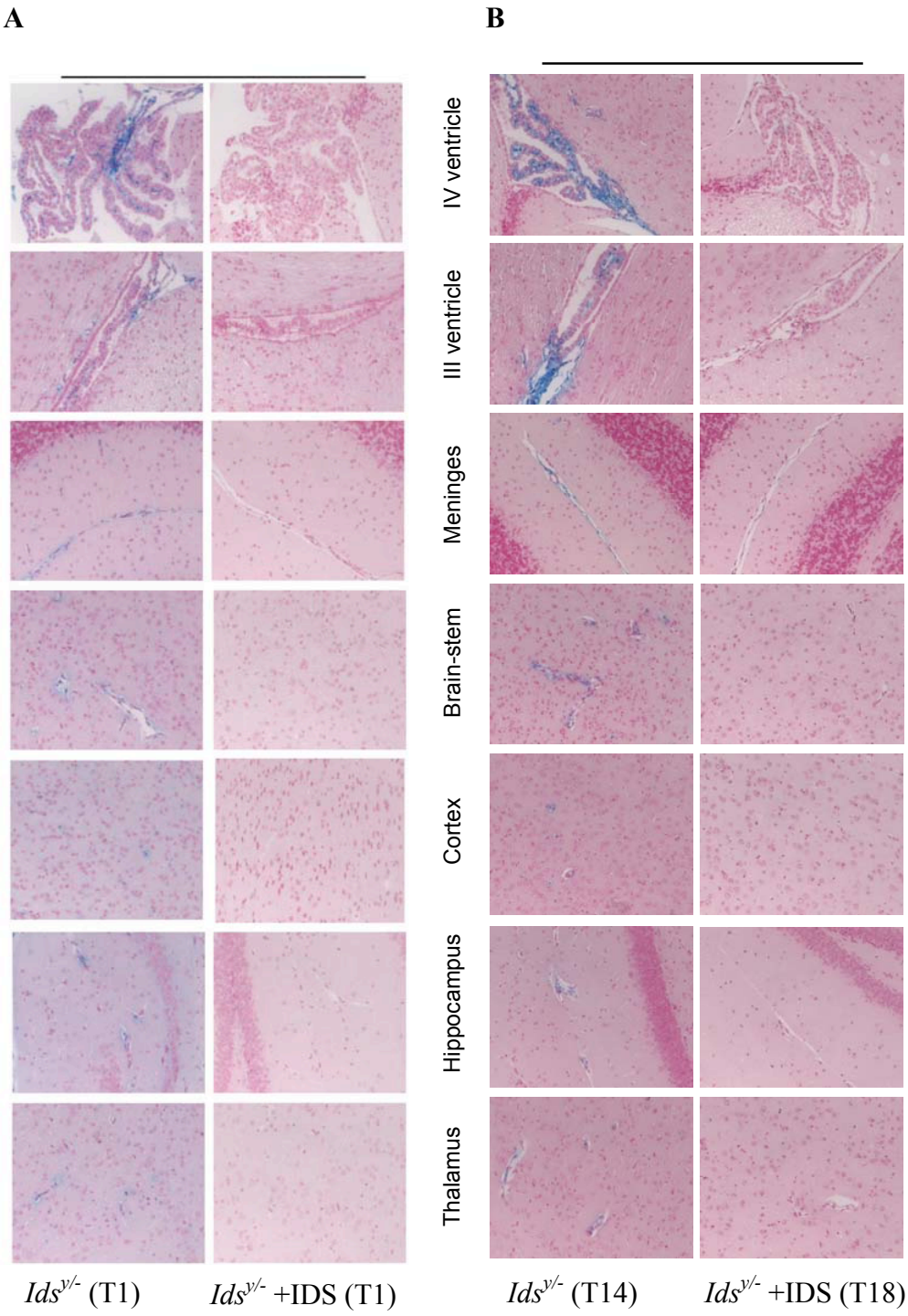

Figure 11. Clearance of GAG Accumulation in *Ids*$^{y/-}$+IDS (T1) and *Ids*$^{y/-}$+IDS (T18) Mice
(A-B) Alcian Blue-stained sections for GAG accumulation in different regions of brains of *Ids*$^{y/-}$ (T1), T14 *Ids*$^{y/-}$ control mice, *Ids*$^{y/-}$+IDS (T1), and T18 AAV2/5CMV-hIDS-injected *Ids*$^{y/-}$ mice. Magnification: 20x.

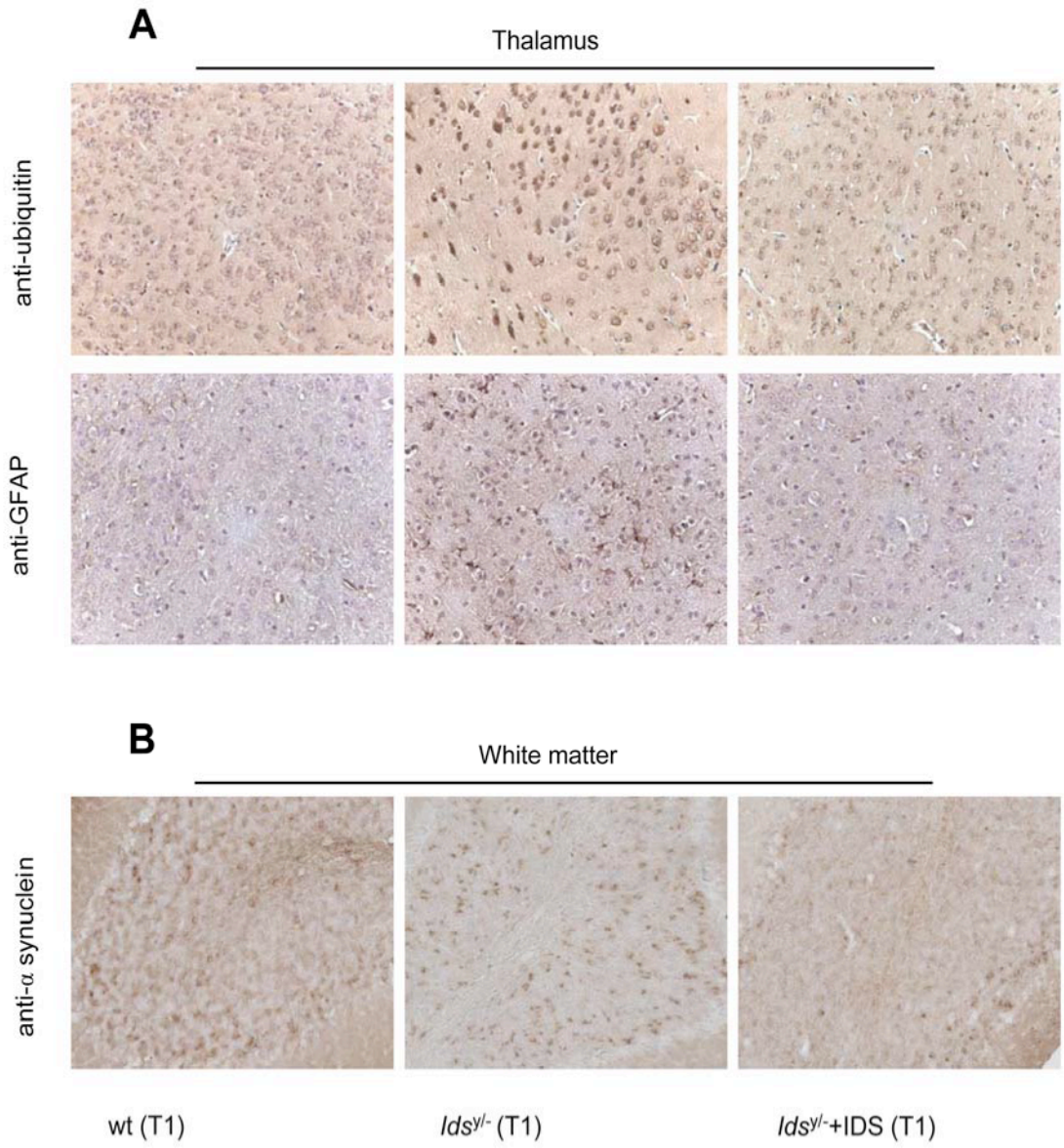

Figure 12. Rescue of Brain Defects in *Ids*$^{y/-}$ Treated T1 Mice
(A) Immunohistochemistry of specific brain markers (anti-ubiquitin, anti-GFAP) in thalamus of wt (T1), *Ids*$^{y/-}$ (T1) and *Ids*$^{y/-}$+IDS (T1) brain sections. **(B)** Immunohistochemistry of anti-α-synuclein in white matter of the same groups of mice. Magnification, 20x.

6. Crossing of Blood-Brain Barrier (BBB) by IDS enzyme

To determine whether the observed GAG clearance and increased IDS activity in the brain of treated MPSII mice were due to the cross of the enzyme through the blood-brain barrier, and not to the transduction of the brain by the viral particles, we analyzed the β-galactosidase activities of the group of wild-type mice (n = 2) that were injected with AAV2/5CMV-LacZ.

Human IDS expression in cDNAs from T1 and T18 tissues was analyzed. No positive expression signals were detected in the brain samples of the control (WT and *Ids*$^{y/-}$) or treated (T1 and T18) mice. In contrast, we found clear amplification of IDS expression in the liver and lungs of both treated groups. For controls, we also amplified mouse Ids transcripts (Figure 13A and Figure 14). For further confirmation of these results, p2 WT mice were injected with 1.0 x 10^{11} AAV2/5CMV-LacZ viral particles. LacZ expression and β-galactosidase activity were seen only in the liver and lungs, not in the brain (Figure 13B). This indicates that both of the hIDS and LacZ transgenes from the AAV2/5 vectors were not expressed in the brains of the injected mice and that, thus, the measured IDS activity was due to IDS uptake from the bloodstream and its crossing of the BBB. Similarly, by using real-time PCR, we could not detect any AAV2/5 viral genomic DNA in the brains of the treated mice, only in their livers, further ruling out crossing of the BBB by AAV2/5 and transduction of the brains (Figure 13C).

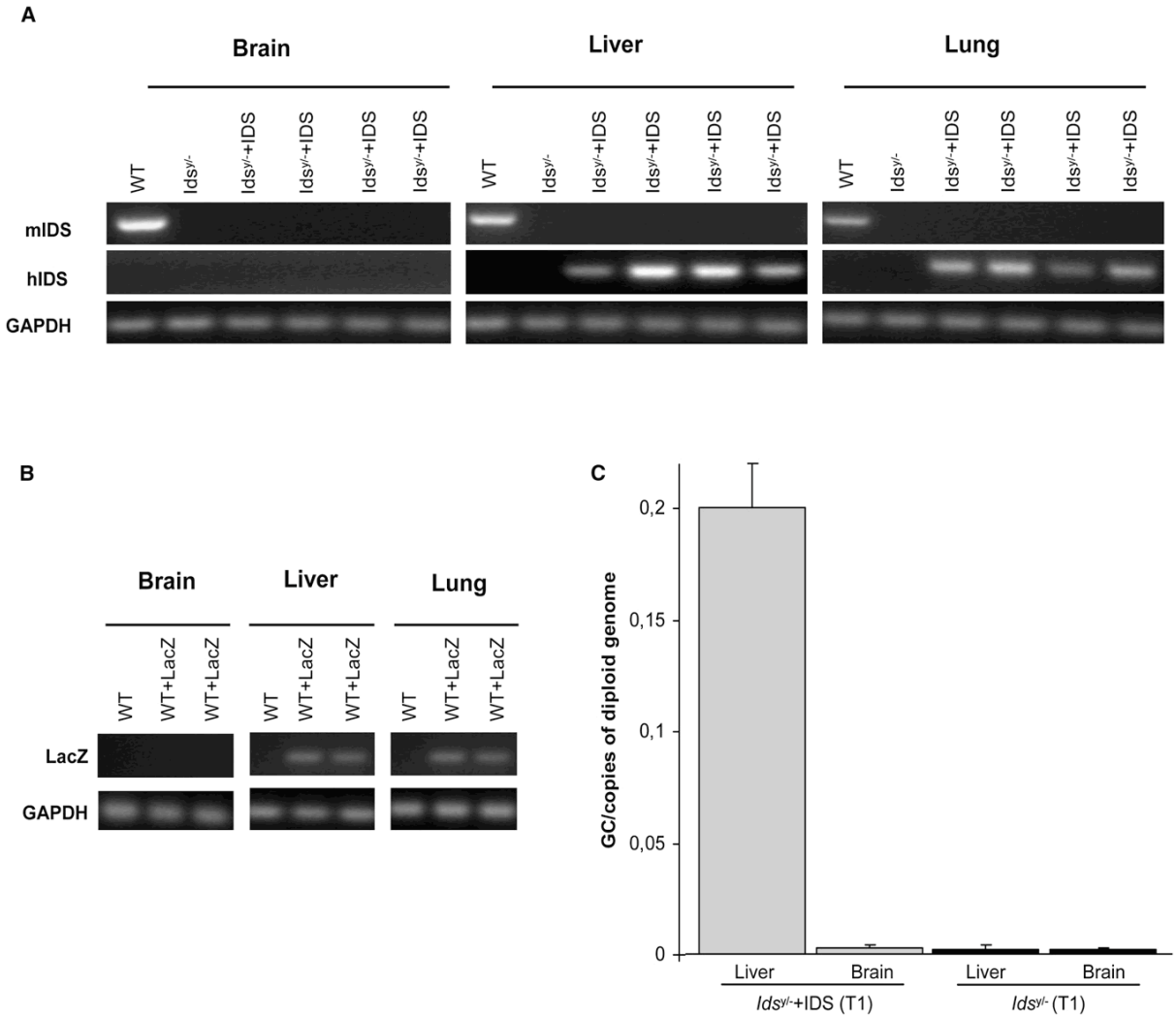

Figure 13. IDS Protein Crossing of the BBB in AAV2/5CMV-hIDS -Injected *Ids*$^{y/-}$ Mice
(A) RT-PCR of IDS from brains, livers, and lungs of T18 WT, T14 *Ids*$^{y/-}$, and T18 *Ids*$^{y/-}$ +IDS mice, for amplification of human and mouse IDS mRNA.
(B) WT mice injected at p2 in the temporal vein with AAV2/5CMV-LacZ and sacrificed after 1 month. RT-PCR of LacZ mRNA from brains, livers, and lungs of T1 WT and T1 WT+LacZ mice. **(C)** Real-time PCR for amplification of viral genomic DNA in brains and livers of T1 nontreated *Ids*$^{y/-}$ mice (n = 4) and T1 AAV2/5CMVhIDS-injected *Ids*$^{y/-}$ mice (n = 4). Error bars indicate standard deviations. $p < 0.05$ (Student's t test).

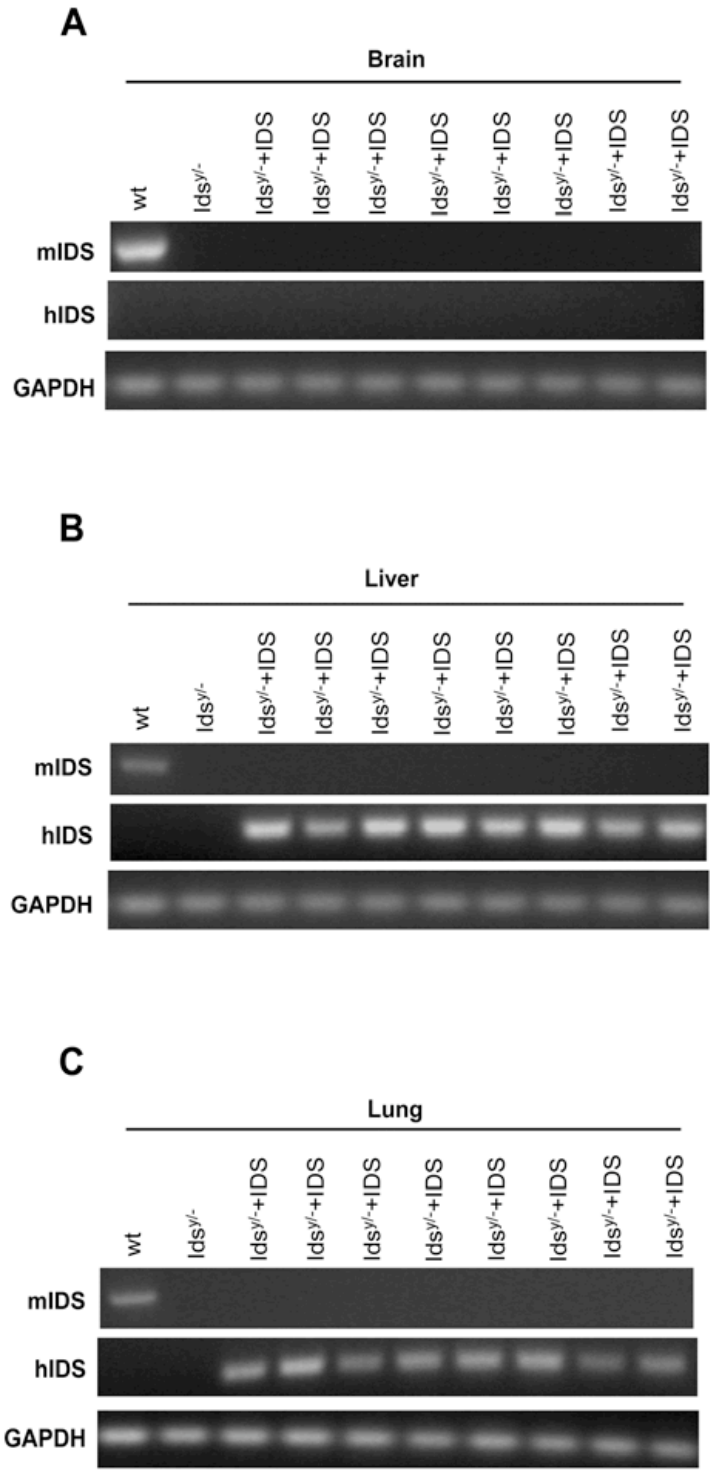

Figure 14. IDS Protein Crossing of the BBB in *Ids*$^{y/-}$+IDS (T1) Injected Mice
(A-C) RT-PCR of hIDS and mIDS mRNAs from brains, livers and lungs of wt (T1), *Ids*$^{y/-}$ (T1), *Ids*$^{y/-}$+IDS (T1) mice.

By contrast, efficient crossing of the BBB was achieved by intravenous injections of the AAV9 vector [54].

In other words, this result confirms that even if the CMV promoter allows expression of the viral particles in some tissues (such as liver and lung), the IDS activity that was measured in the brain is due to the uptake of the enzyme from the blood-brain barrier.

7. Corrections of the locomotor defects in the treated MPSII mice and their performance at the open-field test

The MPSII mice showed drastic skeleton deformation at 4 months of age, which included craniofacial abnormalities, macrodactyly, thickening of the digits and clear craniofacial abnormalities, seen as a short cranium [32].

The treated T18 AAV2/5CMV-hIDS-injected *Ids*$^{y/-}$, untreated and wild-type mice of the same age underwent the open-field test throughout the therapy period to determine horizontal and vertical activities and confirming their improved gross motor phenotype. Figures 15A and 15B show the results of the tests performed at T18. The ability to explore, the locomotion and the anxiety to move of the treated, untreated and wild-type mice were determined.

The mice underwent three trials for 5 min at the end of the therapy (T18). We measured the total distance traveled by the animals during the trial (the number of squares crossed or horizontal activity) and the rearing activity (vertical

activity). The treated MPSII mice behaved as the wild-type ones: they were more active, faster and had no anxiety to explore the space around them; their rearing frequencies, where the mice stood on their hind legs, were also comparable. In contrast, the untreated MPSII mice were much slower and more anxious to explore, and their rearing was poor. Furthermore, the untreated MPSII mice spent a lot of time in the margin area of the field and crossed the center of the open-field apparatus only rarely; in contrast, the treated MPSII mice and the wild-type mice moved fast from the center to the margin area and without hesitation (Figure 15A and figure 15B).

In conclusion, the AAV2/5 IDS gene delivery completely restored the locomotor defects of the MPSII mice.

All in all, these data clearly demonstrates that with only one intravenous systemic injection of AAV2/5CMV-hIDS vector particles administered to newborn p2 *Ids*$^{y/-}$ mice, the mice do not develop the systemic and CNS disease phenotypes up to 18 months of age. We clearly shown that the vector was not transduced in the brains of the treated animals and that the correction of the CNS symptoms was due to the crossing of the BBB by IDS.

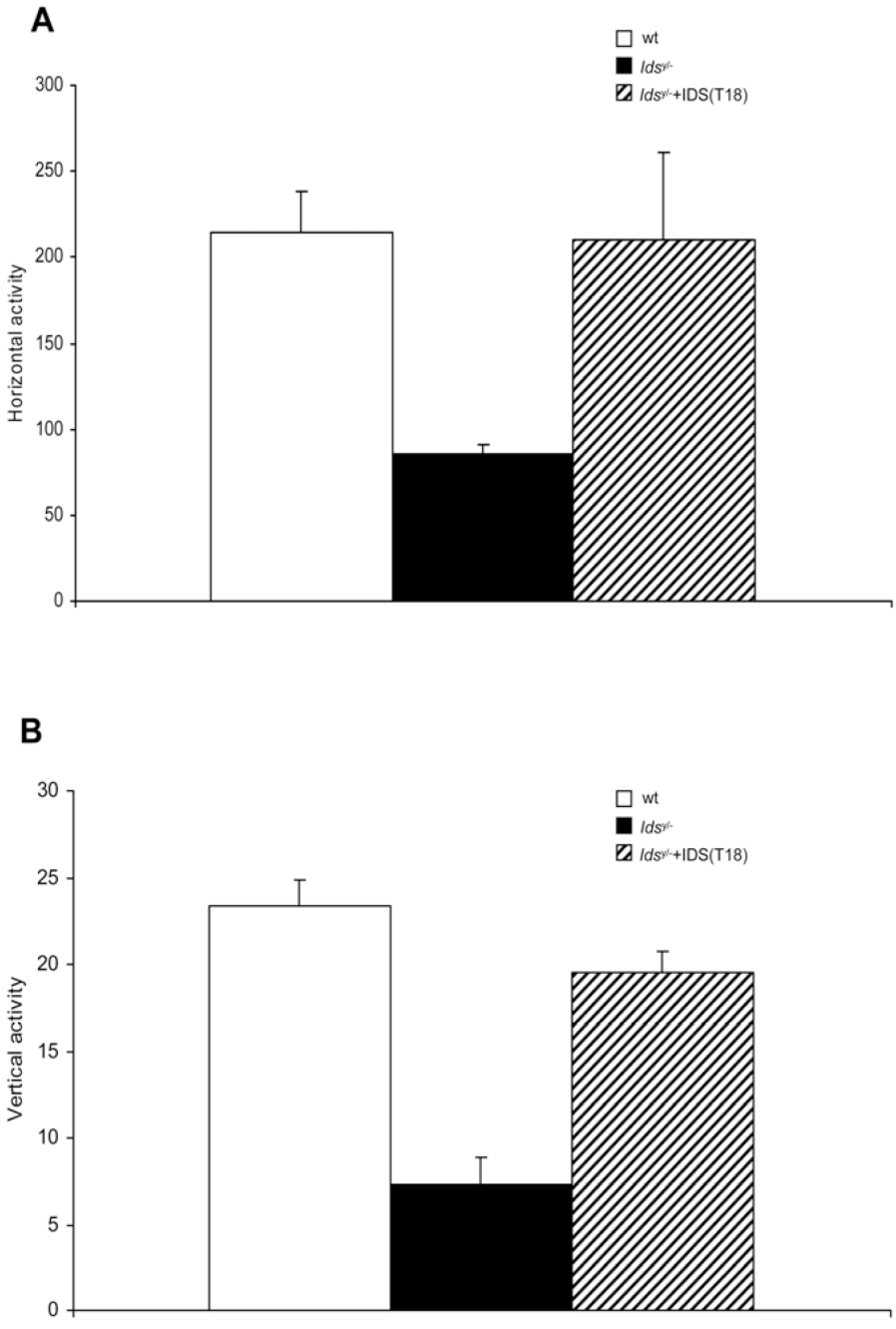

Figure 15. *Ids*$^{y/-}$ Treated Mice Underwent the Open-Field Test
(A, B) Horizontal and vertical activities measured in *Ids*$^{y/-}$+IDS (T18, $n = 4$) and control *Ids*$^{y/-}$ (T14, $n = 3$) mice. The error bars indicate standard deviations. $P < 0.05$ (Student's *t*-test).

DISCUSSION

LSDs, such as Gaucher disease, metachromatic leukodystrophy and MPS, include more than 40 disorders that are caused by defective activities of lysosomal enzymes and that result in the accumulation of undegraded metabolites within the lysosomes.

Most LSDs exist in severe infantile forms that present brain involvement, where the patients die within the first few years of life. There are also adult forms of LSDs that are characterized by the slow development of the peripheral symptoms, which results in physical disabilities. Finally, there are the juvenile forms of intermediate to severe manifestations of LSDs [55]. Although each LSD has a particular clinical and pathological picture, the pathological features can be summarized as neurological symptoms, including seizures, dementia and brainstem dysfunction, and peripheral symptoms, including hepatosplenomegaly, heart and kidney injury, skeleton malformations, muscle atrophy, ocular disease and hearing impairment.

The accumulation of undegraded metabolites within the lysosomes is the primary cause of the disease. However, it has been suggested that the various ranges of clinical symptoms also activate secondary pathways, such as cellular dysfunction, because of the altered activation of biochemical pathways and altered gene expression. Overall, these altered primary and secondary pathways cause tissue pathology and general organ damage [56; 57].

The therapies currently at the stage of preclinical or clinical trials for many of the LSDs are ERT, cellular therapies, such as BMT, and virus-mediated gene therapy.

The choice between these three therapeutic approaches relates to their different efficacies with respect to the different LSDs. In particular, for the treatment of MPSII, or Hunter syndrome, which is characterized by the inactivity of the IDS enzyme and the consequent accumulation of heparan and dermatan sulfates (GAGs) within the lysosomes, at present, ERT and BMT result in doubtful prognoses for prolonged positive outcomes [58-61]. Attempts of therapy for MPSII are palliative and focused on management of the clinical symptoms. This is also due to the limited number of patients under treatment and to their short length of follow-up. Moreover, in the ERT, the patients receive weekly expensive injection of IDS enzyme; these repeated administrations at long run could cause an immuno-response against IDS protein, reversing the therapeutic effect. Additionally, the ERT protocol is able to partially rescue the visceral phenotype of MPSII patients, but not the CNS one.

Thus, as a mouse model for MPSII is available, we have designed an efficient gene-therapy protocol.

We have investigated the MPSII mouse model for its gross phenotypic characteristics and metabolic defects. Furthermore, we analyzed neuropathological features within the CNS.

Then, we systemically delivered the IDS gene into the temporal vein using AAV2/5 vectors. We have been able to specifically transduce some tissues (such as the liver and the lung) and to promote the production of human IDS in these tissues. The enzyme was then secreted efficiently into the blood stream, and it targeted all of the nontransduced tissues with great efficiency. Complete correction of the visceral, CNS and locomotor defects was achieved.

A partial rescue of the IDS activity in the CNS was also observed. The AAV vectors [62] transduce murine tissues efficiently and their production allows the exchange of the surface proteins (the capsid) between different serotypes [51; 52; 63-65]. The hybrid vectors contain the genome packaged in capsids from different AAV serotypes and detain effective transduction characteristics, resulting in excellent efficacy of gene expression and tissue tropism. In fact, AAV2/1 and 2/7 vectors transduce muscle very powerfully [41; 64; 65], AAV2/5 tranduces lung by entering the airway from the apical side and other tissues [51; 52; 66] and AAV2/8 is the most efficient AAV vector for liver-directed gene transfer [41].

We used the CMV promoter to express the IDS gene; this is a ubiquitous promoter. Thus, the combination of AAV5 and the CMV promoter was extremely useful for the production of high levels of the circulating IDS enzyme and could represent a valuable tool for the treatment of MPSII patients.

Usually, the correction of MPS defects can be achieved by restoring the enzymatic activities to up to only 1–10% of their normal levels [67]; in the present

study, we have restored the IDS activity with respect to the normal wild-type levels. We injected the viral particles at 1.0 x 10^{11} per kilogram in our experiments and we were able to obtain high levels of IDS in the plasma, which ranged 5 times higher than the normal wild-type values.

For the future, this is a valuable concept, as it should scale down the amounts of viral particles that might be needed in the treatment of larger animals and of humans in clinical trials.

In this study, the high levels of the circulating IDS enzyme have resulted in its crossing of the hemato-encephalic barrier, leading to a partial rescue of the IDS deficiency, along with the complete clearance of the GAGs in different regions of brain and complete rescue of neurodegenerative defects.

In this thesis, the crossing of BBB has represented a crucial and necessary point. In fact, the major limit in the treatment and cure of most neurodegenerative diseases, is just the cross of BBB that surround and protect the brain [68].

Although at present it is still unknown how IDS crosses the BBB, the long half-life of circulating IDS, as shown by its slow clearance from the blood (high plasma levels in treated animals), probably allows the enzyme to cross the BBB. Interestingly, chemically modified β -glucuronidase showed slower plasma clearance, and the modified enzyme efficiently crossed the BBB after its systemic infusion in MPSVII mice [69].

Partial correction of CNS defects has been described in a mouse model of MPSVII after intrahepatic administration of AAV2 vectors [50]. Furthermore, a therapeutic effect in the brain has also been shown by administration of high doses of enzyme through ERT. Both β-glucuronidase and α-mannosidase were able to cross the hemato-encephalic barrier in MPSVII and in α-mannosidosis mouse models, respectively [47; 48].

Whether high circulating levels of IDS are required for its delivery through receptor-mediated uptake or via different routes, such as pinocytosis or transcytosis, remains an open question. MPSII patients affected by the severe form of the disease ideally need to be treated with one administration of the vector that can rescue both visceral and CNS defects.

Nevertheless, these findings have demonstrated that high circulating levels of the IDS enzyme, coupled with very early treatment of the mice, provide an effective therapy for MPSII in all of the affected tissues. Potentially, modulation of the physical parameters of the enzymes, such as their stability, and early vector administration might be useful approaches for the treatment of other lysosomal-storage disorders.

In conclusion, the systemic delivery of IDS through AAV2/5 vectors is highly efficient and represents a promising approach for future applications in the therapy of MPSII patients.

Furthermore, it can be considered as proof of principle for the treatment of LSDs including other sulfatase deficits, in particular for those diseases that involve the CNS. The systemic distribution of the active enzyme might represent an efficient way of delivery for many of the metabolic disorders affecting different tissues and brain.

REFERENCES

1. Braulke T, Bonifacino JS (2009) Sorting of lysosomal proteins. Biochim Biophys Acta 1793:605-614

2. E. van Meel JK (2008) Imaging and imagination: understanding the endolysosomal system. Cell Biol 129 (2008) 253–266

3. D. Lazzarino CG (1989) Mannose processing is an important determinant in the assembly of phosphorylated high mannose-type oligosaccharides. J Biol Chem 264 5015–5023

4. Neufeld EF, Muenzer J (2001) The mucopolysaccharidoses. In: Scriver CR, Beaudet AL, Sly WS, Valle D (eds) The metabolic and molecular basis of inherited disease. Mc Graw-Hill, New York, pp 3421-3452

5. Meikle PJ, Hopwood JJ, Clague AE, Carey WF (1999) Prevalence of lysosomal storage disorders. Jama 281:249-254

6. Sandhoff K (2001) The GM2-gangliosidoses and the elucidation of the beta-hexosaminidase system. Advances in genetics 44:67-91

7. von Figura K, Schmidt B, Selmer T, Dierks T (1998) A novel protein modification generating an aldehyde group in sulfatases: its role in catalysis and disease. BioEssays 20:505-510

8. Meikle PJ, Ranieri E, Ravenscroft EM, Hua CT, Brooks DA, Hopwood JJ (1999) Newborn screening for lysosomal storage disorders. The Southeast Asian journal of tropical medicine and public health 30 Suppl 2:104-110

9. Parenti G, Meroni G, Ballabio A (1997) The sulfatase gene family. Curr Opin Genet Dev 7:386-391

10. Hopwood JJ, Ballabio A (2001) Multiple sulfatase deficiency and the nature of the sulfatase family. In: Scriver CR, Beaudet AL, Valle D, Sly WS (eds) The metabolic and molecular basis of inherited disease. Mc Graw-Hill, New York, pp 3725-3732

11. Meroni G, Franco B, Archidiacono N, Messali S, Andolfi G, Rocchi M, Ballabio A (1996) Characterization of a cluster of sulfatase genes on Xp22.3 suggests gene duplications in an ancestral pseudoautosomal region. Hum Mol Genet 5:423-431

12. Bond CS, Clements PR, Ashby SJ, Collyer CA, Harrop SJ, Hopwood JJ, Guss JM (1997) Structure of a human lysosomal sulfatase. Structure 5:277-289.

13. Lukatela G, Krauss N, Theis K, Selmer T, Gieselmann V, von Figura K, Saenger W (1998) Crystal structure of human arylsulfatase A: the aldehyde function and the metal ion at the active site suggest a novel mechanism for sulfate ester hydrolysis. Biochemistry 37:3654-3664.

14. Schmidt B, Selmer T, Ingendoh A, von Figura K (1995) A novel amino acid modification in sulfatases that is defective in multiple sulfatase deficiency. Cell 82:271-278

15. Fey J, Balleininger M, Borissenko LV, Schmidt B, von Figura K, Dierks T (2001) Characterization of posttranslational formylglycine formation by luminal components of the endoplasmic reticulum. J Biol Chem 276:47021-47028.

16. Dierks T, Miech C, Hummerjohann J, Schmidt B, Kertesz MA, von Figura K (1998) Posttranslational formation of formylglycine in prokaryotic sulfatases by modification of either cysteine or serine. J Biol Chem 273:25560-25564.

17. Schirmer A, Kolter R (1998) Computational analysis of bacterial sulfatases and their modifying enzymes. Chem Biol 5:R181-186.

18. Ferrante P, Messali S, Meroni G, Ballabio A (2002) Molecular and Biochemical characterisation of a novel sulphatase gene: Arylsulfatase G (ARSG). European Journal of Human Genetics 10:813-818

19. Morimoto-Tomita M, Uchimura K, Werb Z, Hemmerich S, Rosen SD (2002) Cloning and characterization of two extracellular heparin-degrading endosulfatase in mice and humans. The Journal of Biological Chemistry 277:49175-49185

20. Franco B, Meroni G, Parenti G, Levilliers J, Bernard L, Gebbia M, Cox L, Maroteaux P, Sheffield L, Rappold GA, Andria G, Petit C, Ballabio A (1995) A cluster of sulfatase genes on Xp22.3: mutations in chondrodysplasia punctata (CDPX) and implications for warfarin embryopathy. Cell 81:15-25

21. Von Figura K, Gieselmann V, Jaeken J (2001) Metachromatic leukodystrophy. In: Scriver CR, Beaudet AL, Sly WS, Valle D (eds) The

metabolic and molecular basis of inherited disease. Mc Graw-Hill, New York, pp 3695-3724

22. Austin J (1966) Studies in metachromatic leukodystrophy XII. Multiple sulfatase deficiency. Arch Neurol 15:13-28

23. Kolodny EH, Fluharty AL (1995) Metachromatic leukodystrophy and multiple sulfatase deficiency: sulfatide lipidosis. In: Scriver CR, Beaudet AL, Sly WS, Valle D (eds) The Metabolic and Molecular Bases of Inherited Disease. McGraw-Hill, New York, pp 2693-2741

24. Cosma MP, Pepe S, Annunziata I, Newbold RF, Grompe M, Parenti G, Ballabio A (2003) The multiple sulfatase deficiency gene encodes an essential and limiting factor for the activity of sulfatases. Cell 113:445-456

25. Dierks T, Schmidt B, Borissenko LV, Peng J, Preusser A, Mariappan M, von Figura K (2003) Multiple Sulfatase Deficiency Is Caused by Mutations in the Gene Encoding the Human C(alpha)-Formylglycine Generating Enzyme. Cell 113:435-444

26. Hopwood JJ, Bunge S, Morris CP, Wilson PJ, Steglich C, Beck M, Schwinger E, Gal A (1993) Molecular basis of mucopolysaccharidosis type II: mutations in the iduronate-2-sulphatase gene. Hum Mutat 2:435-442

27. Neufeld EF, Muenzer J (1995) The mucopolysaccharidoses. In: Scriver CR, Beaudet AL, Sly WS, Valle D (eds) The Metabolic and Molecular Bases of Inherited Disease. McGraw-Hill, New York, pp 2465-2494

28. Spranger J (1972) The systemic mucopolysaccharidoses. Ergebnisse der inneren Medizin und Kinderheilkunde 32:165-265

29. Young ID, Harper PS (1982) Incidence of Hunter's syndrome. Human genetics 60:391-392

30. Fowler GW, Sukoff M, Hamilton A, Williams JP (1975) Communicating hydrocephalus in children with genetic inborn errors of metabolism. Child's brain 1:251-254

31. Muenzer J, Lamsa JC, Garcia A, Dacosta J, Garcia J, Treco DA (2002) Enzyme replacement therapy in mucopolysaccharidosis type II (Hunter syndrome): a preliminary report. Acta Paediatr Suppl 91:98-99

32. Cardone M, Polito VA, Pepe S, Mann L, D'Azzo A, Auricchio A, Ballabio A, Cosma MP (2006) Correction of Hunter syndrome in the MPSII mouse model by AAV2/8-mediated gene delivery. Hum Mol Genet 15:1225-1236

33. Kay MA, Glorioso JC, Naldini L (2001) Viral vectors for gene therapy: the art of turning infectious agents into vehicles of therapeutics. Nature medicine 7:33-40

34. Linden RM, Ward P, Giraud C, Winocour E, Berns KI (1996) Site-specific integration by adeno-associated virus. Proceedings of the National Academy of Sciences of the United States of America 93:11288-11294

35. Bennett J, Maguire AM, Cideciyan AV, Schnell M, Glover E, Anand V, Aleman TS, Chirmule N, Gupta AR, Huang Y, Gao GP, Nyberg WC, Tazelaar J, Hughes J, Wilson JM, Jacobson SG (1999) Stable transgene expression in rod photoreceptors after recombinant adeno-associated virus-mediated gene transfer to monkey retina. Proceedings of the National Academy of Sciences of the United States of America 96:9920-9925.

36. Hermonat PL, Santin AD, Carter CA, Parham GP, Quirk JG (1997) Multiple cellular proteins are recognized by the adeno-associated virus Rep78 major regulatory protein and the amino-half of Rep78 is required for many of these interactions. Biochemistry and molecular biology international 43:409-420

37. Kotin RM, Linden RM, Berns KI (1992) Characterization of a preferred site on human chromosome 19q for integration of adeno-associated virus DNA by non-homologous recombination. The EMBO journal 11:5071-5078

38. Samulski RJ, Zhu X, Xiao X, Brook JD, Housman DE, Epstein N, Hunter LA (1991) Targeted integration of adeno-associated virus (AAV) into human chromosome 19. The EMBO journal 10:3941-3950

39. Lai YK, Shen WY, Brankov M, Lai CM, Constable IJ, Rakoczy PE (2002) Potential long-term inhibition of ocular neovascularisation by recombinant adeno-associated virus-mediated secretion gene therapy. Gene Ther 9:804-813.

40. Auricchio A, Hildinger M, O'Connor E, Gao GP, Wilson JM (2001) Isolation of Highly Infectious and Pure Adeno-Associated Virus Type 2 Vectors with a Single-Step Gravity-Flow Column. Hum Gene Ther 12:71-76.

41. Gao GP, Alvira MR, Wang L, Calcedo R, Johnston J, Wilson JM (2002) Novel adeno-associated viruses from rhesus monkeys as vectors for human gene therapy. Proceedings of the National Academy of Sciences of the United States of America 99:11854-11859

42. Gao G, Qu G, Burnham MS, Huang J, Chirmule N, Joshi B, Yu QC, Marsh JA, Conceicao CM, Wilson JM (2000) Purification of recombinant adeno-associated virus vectors by column chromatography and its performance in vivo. Hum Gene Ther 11:2079-2091.

43. Voznyi YV, Keulemans JL, van Diggelen OP (2001) A fluorimetric enzyme assay for the diagnosis of MPS II (Hunter disease). J Inherit Metab Dis 24:675-680

44. de Jong JG, Wevers RA, Laarakkers C, Poorthuis BJ (1989) Dimethylmethylene blue-based spectrophotometry of glycosaminoglycans in untreated urine: a rapid screening procedure for mucopolysaccharidoses. Clin Chem 35:1472-1477

45. Bronikowski AM, Carter PA, Swallow JG, Girard IA, Rhodes JS, Garland T, Jr. (2001) Open-field behavior of house mice selectively bred for high voluntary wheel-running. Behav Genet 31:309-316

46. Hawkins BT, Davis TP (2005) The blood-brain barrier/neurovascular unit in health and disease. Pharmacol Rev 57:173-185

47. Roces DP, Lullmann-Rauch R, Peng J, Balducci C, Andersson C, Tollersrud O, Fogh J, Orlacchio A, Beccari T, Saftig P, von Figura K (2004) Efficacy of enzyme replacement therapy in alpha-mannosidosis mice: a preclinical animal study. Hum Mol Genet 13:1979-1988

48. Vogler C, Levy B, Grubb JH, Galvin N, Tan Y, Kakkis E, Pavloff N, Sly WS (2005) Overcoming the blood-brain barrier with high-dose enzyme replacement therapy in murine mucopolysaccharidosis VII. Proceedings of the National Academy of Sciences of the United States of America 102:14777-14782

49. Matzner U, Lullmann-Rauch R, Stroobants S, Andersson C, Weigelt C, Eistrup C, Fogh J, D'Hooge R, Gieselmann V (2009) Enzyme replacement improves ataxic gait and central nervous system histopathology in a mouse model of metachromatic leukodystrophy. Mol Ther 17:600-606

50. Sferra TJ, Backstrom K, Wang C, Rennard R, Miller M, Hu Y (2004) Widespread correction of lysosomal storage following intrahepatic injection of a recombinant adeno-associated virus in the adult MPS VII mouse. Mol Ther 10:478-491

51. Hildinger M, Auricchio A, Gao G, Wang L, Chirmule N, Wilson JM (2001) Hybrid vectors based on adeno-associated virus serotypes 2 and 5 for muscle-directed gene transfer. J Virol 75:6199-6203.

52. Auricchio A, O'Connor E, Weiner D, Gao GP, Hildinger M, Wang L, Calcedo R, Wilson JM (2002) Noninvasive gene transfer to the lung for systemic delivery of therapeutic proteins. J Clin Invest 110:499-504

53. Suzuki K, Iseki E, Togo T, Yamaguchi A, Katsuse O, Katsuyama K, Kanzaki S, Shiozaki K, Kawanishi C, Yamashita S, Tanaka Y, Yamanaka S, Hirayasu Y (2007) Neuronal and glial accumulation of alpha- and beta-synucleins in human lipidoses. Acta Neuropathol 114:481-489

54. Foust KD, Nurre E, Montgomery CL, Hernandez A, Chan CM, Kaspar BK (2009) Intravascular AAV9 preferentially targets neonatal neurons and adult astrocytes. Nat Biotechnol 27:59-65

55. Wraith JE (2002) Lysosomal disorders. Semin Neonatol 7:75-83

56. Futerman AH, van Meer G (2004) The cell biology of lysosomal storage disorders. Nat Rev Mol Cell Biol 5:554-565

57. Fratantoni JC, Hall CW, Neufeld EF (1968) Hurler and Hunter syndromes: mutual correction of the defect in cultured fibroblasts. Science 162:570-572

58. Brady RO, Schiffmann R (2004) Enzyme-replacement therapy for metabolic storage disorders. Lancet Neurol 3:752-756

59. Li P, Thompson JN, Hug G, Huffman P, Chuck G (1996) Biochemical and molecular analysis in a patient with the severe form of Hunter syndrome after bone marrow transplantation. Am J Med Genet 64:531-535

60. Coppa GV, Gabrielli O, Zampini L, Pierani P, Giorgi PL, Jezequel AM, Orlandi F, Miniero R, Busca A, De Luca T, et al. (1995) Bone marrow transplantation in Hunter syndrome (mucopolysaccharidosis type II): two-year follow-up of the first Italian patient and review of the literature. Pediatr Med Chir 17:227-235

61. Peters C, Krivit W (2000) Hematopoietic cell transplantation for mucopolysaccharidosis IIB (Hunter syndrome). Bone Marrow Transplant 25:1097-1099

62. Monahan PE, Samulski RJ (2000) Adeno-associated virus vectors for gene therapy: more pros than cons? [In Process Citation]. Mol Med Today 6:433-440

63. Auricchio A, Kobinger G, Anand V, Hildinger M, O'Connor E, Maguire AM, Wilson JM, Bennett J (2001) Exchange of surface proteins impacts on viral vector cellular specificity and transduction characteristics: the retina as a model. Human Molecular Genetics 10:3075-3081

64. Chao H, Liu Y, Rabinowitz J, Li C, Samulski RJ, Walsh CE (2000) Several log increase in therapeutic transgene delivery by distinct adeno-associated viral serotype vectors. Mol Ther 2:619-623.

65. Rabinowitz JE, Rolling F, Li C, Conrath H, Xiao W, Xiao X, Samulski RJ (2002) Cross-packaging of a single adeno-associated virus (AAV) type 2 vector genome into multiple AAV serotypes enables transduction with broad specificity. J Virol 76:791-801.

66. Zabner J, Seiler M, Walters R, Kotin RM, Fulgeras W, Davidson BL, Chiorini JA (2000) Adeno-associated virus type 5 (AAV5) but not AAV2 binds to the apical surfaces of airway epithelia and facilitates gene transfer. J Virol 74:3852-3858.

67. Cheng SH, Smith AE (2003) Gene therapy progress and prospects: gene therapy of lysosomal storage disorders. Gene Ther 10:1275-1281

68. Sands MS, Haskins ME (2008) CNS-directed gene therapy for lysosomal storage diseases. Acta Paediatr Suppl 97(457):22-7. Review.

69. Grubb JH, Vogler C, Levy B, Galvin N, Tan Y, Sly WS (2008) Chemically modified beta-glucuronidase crosses blood-brain barrier and clears

neuronal storage in murine mucopolysaccharidosis VII. Proceedings of the National Academy of Sciences of the United States of America 105:2616-2621

AKNOWLEDGEMENTS

Dedicato alla mia famiglia, a mio padre, mia madre e mio fratello Marco che mi hanno guidato, supportato e dato la possibilita' di raggiungere i miei obiettivi. Una ulteriore dedica a Francesco, che mi e' sempre e costantemente rimasto accanto in questi ultimi anni, che ha creduto in me e ha saputo darmi forza nei momenti di maggiore difficolta'; la persona che con grande intelligenza mi sostiene lasciandomi la liberta' di sognare.

I would like to thank at first my three supervisors: Dr. Maria Pia Cosma, who gave me the great possibility to join to her group and to work in a very good institute such as TIGEM; Prof. Andrea Ballabio, who accepted the co-supervisor engagement contributing to the realization of this work; Prof. Mark Haskins, who gave me with great patience some useful and important suggestions for my final work. I was honored of working with them who are brilliant scientists and good persons.

I thank also Sara Salvia, Edoardo Nusco and Monica Doria, for their great technical support. Thanks to the people of the informatics core at TIGEM and especially to Giampiero Lago, who was always available for helping me with any kind of trouble and for the friendship which he demonstrated to me.

I would like to give a special thank to the friends who supported me even with a simple smile and whom I shared my daily life at TIGEM: Alda Graziano, Filippo Menolascina and Maria Aurelia Ricci.

A special thank is for two important persons: Serena Abbondante and Irene Cantone; they became for me two of my best friends sharing happiness and sorrow, successes and failures. In particular, Irene was able to increase in me the capacity to believe into myself and to dream.

Thank to my family and to Francesco Ponza that believed in me always and encouraged me in all the choices that I taken. Their presence was constant and irreplaceable for the reaching of my objectives.